1 Structure of the observables

Let us start from Eq. (2.6) of Ref. [1], that is the fully differential cross section for lepton-pair production in the region in which the TMD factorisation applies, *i.e.* $q_T \ll Q$. After some minor manipulations, it reads:

$$\frac{d\sigma}{dQdydq_T} = \frac{16\pi\alpha^2 q_T}{9Q^3} H(Q,\mu) \sum_q C_q(Q) \int \frac{d^2\mathbf{b}}{4\pi} e^{i\mathbf{b}\cdot\mathbf{q}_T} \overline{F}_q(x_1,\mathbf{b};\mu,\zeta)\overline{F}_{\bar{q}}(x_2,\mathbf{b};\mu,\zeta)\,, \tag{1}$$

where Q, y, and q_T are the invariant mass, the rapidity, and the transverse momentum of the lepton pair, respectively, while α is the electromagnetic coupling, H is the appropriate QCD hard factor that can be perturbatively computed, and C_q are the effective electroweak charges. In addition, the variables x_1 and x_2 are functions of Q and y and are given by:

$$x_{1,2} = \frac{Q}{\sqrt{s}} e^{\pm y}\,, \tag{2}$$

being $\sqrt{s}$ the centre-of-mass energy of the collision. In Eq. (1) we are using the short-hand notation:

$$\overline{F}_q(x,\mathbf{b};\mu,\zeta) \equiv x F_q(x,\mathbf{b};\mu,\zeta)\,, \tag{3}$$

that is convenient for the implementation. The scales μ and ζ are introduced as a consequence of the removal of UV and rapidity divergences in the definition of the TMDs. Despite these scales are arbitrary scales, they are typically chosen $\mu = \sqrt{\zeta} = Q$. Therefore, for all practical purposes their presence is fictitious.

The computation-intensive part of Eq.(1) has the form of the integral:

$$I_{ij}(x_1,x_2,q_T;\mu,\zeta) = \int \frac{d^2\mathbf{b}}{4\pi} e^{i\mathbf{b}\cdot\mathbf{q}_T} \overline{F}_i(x_1,\mathbf{b};\mu,\zeta)\overline{F}_j(x_2,\mathbf{b};\mu,\zeta)\,. \tag{4}$$

where $\overline{F}_{i(j)}$ are combinations of evolved TMD PDFs. At this stage, for convenience, i and j do not coincide with q and $\bar{q}$ but they are linked through a simple linear transformation. The integral over the bidimensional impact parameter $\mathbf{b}$ has to be taken. However, $\overline{F}_{i(j)}$ only depend on the absolute value of $\mathbf{b}$, therefore Eq. (4) can be written as:

$$I_{ij}(x_1,x_2,q_T;\mu,\zeta) = \frac{1}{2}\int_0^\infty db\, b J_0(bq_T)\overline{F}_i(x_1,b;\mu,\zeta)\overline{F}_j(x_2,b;\mu,\zeta)\,. \tag{5}$$

where J_0 is the zero-th order Bessel function of the first kind whose integral representation is:

$$J_0(x) = \frac{1}{2\pi}\int_0^{2\pi} d\theta e^{ix\cos(\theta)}\,. \tag{6}$$

The evolved quark TMD PDF $\overline{F}_i$ at the final scales μ and ζ is obtained by multiplying the same distribution at the initial scales μ_0 and ζ_0 by a single evolution factor R_q([1]). that is:

$$\overline{F}_i(x,b;\mu,\zeta) = R_q(\mu_0,\zeta_0\to\mu,\zeta;b)\overline{F}_i(x,b;\mu_0,\zeta_0)\,. \tag{7}$$

The initial scale TMD PDFs at small values b can be written as:

$$\overline{F}_i(x,b;\mu_0,\zeta_0) = \sum_{j=g,q(\bar{q})} x\int_x^1 \frac{dy}{y} C_{ij}(y;\mu_0,\zeta_0) f_j\left(\frac{x}{y},\mu_0\right)\,, \tag{8}$$

where f_j are the collinear PDFs (including the gluon) and C_{ij} are the so-called matching functions that are perturbatively computable and are currently known to NNLO, *i.e.* $\mathcal{O}(\alpha_s^2)$. If we define:

$$\overline{f}_i(x,\mu_0) = x f_i(x,\mu_0)\,, \tag{9}$$

[1]Note that in Eq. (1) the gluon TMD PDF $\overline{F}_g$ is not involved. If also the gluon TMD PDF was involved, it would evolve by means of a different evolution factor R_g.

Eq. (8) can be written as:

$$\overline{F}_i(x,b;\mu_0,\zeta_0) = \sum_{j=g,q(\bar{q})} \int_x^1 dy\, C_{ij}(y;\mu_0,\zeta_0)\overline{f}_i\left(\frac{x}{y},\mu_0\right) . \tag{10}$$

Putting Eqs. (7) and (10), one finds:

$$\overline{F}_i(x,b;\mu,\zeta) = R_q(\mu_0,\zeta_0\to\mu,\zeta;b) \sum_{j=g,q(\bar{q})} \int_x^1 dy\, C_{ij}(y;\mu_0,\zeta_0)\overline{f}_i\left(\frac{x}{y},\mu_0\right) . \tag{11}$$

Matching and evolution are affected by non-perturbative effects that become relevant at large b. In order to account for such effects, one usually introduces a phenomenological function $f_{\rm NP}$. In the traditional approach (CSS [2]), the b-space TMDs get a multiplicative correction that does not depend on the flavour. In addition, the perturbative content of the TMDs is smoothly damped away at large b by introducing the so-called b_*-prescription:

$$\overline{F}_i(x,b;\mu,\zeta) \to \overline{F}_i(x,b_*(b);\mu,\zeta) f_{\rm NP}(x,b,\zeta) , \tag{12}$$

where $b_* \equiv b_*(b)$ is a monotonic function of the impact parameter b such that:

$$\lim_{b\to 0} b_*(b) = b_{\rm min} \quad \text{and} \quad \lim_{b\to\infty} b_*(b) = b_{\rm max} , \tag{13}$$

being $b_{\rm min}$ and $b_{\rm max}$ constant values both in the perturbative region. Including the non-perturbative function, Eq. (5) becomes:

$$\begin{aligned} I_{ij}(x_1,x_2,q_T;\mu,\zeta) &= \int_0^\infty db\, J_0(bq_T)\left[\frac{b}{2}\overline{F}_i(x_1,b_*(b);\mu,\zeta)\overline{F}_j(x_2,b_*(b);\mu,\zeta) f_{\rm NP}(x_1,b,\zeta) f_{\rm NP}(x_2,b,\zeta)\right] \\ &= \frac{1}{q_T}\int_0^\infty d\bar{b}\, J_0(\bar{b})\left[\frac{\bar{b}}{2q_T}\overline{F}_i(x_1,b_*\left(\frac{\bar{b}}{q_T}\right);\mu,\zeta)\overline{F}_j(x_2,,b_*\left(\frac{\bar{b}}{q_T}\right);\mu,\zeta) f_{\rm NP}\left(x_1,\frac{\bar{b}}{q_T},\zeta\right) f_{\rm NP}\left(x_2,\frac{\bar{b}}{q_T},\zeta\right)\right] . \end{aligned} \tag{14}$$

Eq. (14) is a Hankel tranform and can be efficiently computed using the so-called Ogata quadrature [3]. Effectively, the computation of the integral in Eq. (4) is achieved through a weighted sum:

$$\begin{aligned} I_{ij}(x_1,x_2,q_T;\mu,\zeta) \;\simeq\; & \frac{1}{q_T}\sum_{n=1}^{N} \frac{w_n^{(0)} z_n^{(0)}}{2q_T}\overline{F}_i\left(x_1,b_*\left(\frac{z_n^{(0)}}{q_T}\right);\mu,\zeta\right)\overline{F}_j\left(x_2,b_*\left(\frac{z_n^{(0)}}{q_T}\right);\mu,\zeta\right) \\ \times\; & f_{\rm NP}\left(x_1,\frac{z_n^{(0)}}{q_T},\zeta\right) f_{\rm NP}\left(x_2,\frac{z_n^{(0)}}{q_T},\zeta\right) , \end{aligned} \tag{15}$$

where the unscaled coordinates $z_n^{(0)}$ and the weights $w_n^{(0)}$ can be precomputed in terms of the zero's of the Bessel function J_0 and one single parameter (see Ref. [3] for more details, specifically Eqs. (5.1) and (5.2) or Appendix A for the relevant formula to compute the unscaled coordinates and the weights)[2]. Based on the (empirically verified) assumption that the absolute value of each term in the sum in the r.h.s. of Eq. (15) is smaller than that of the preceding one, the truncation number N is chosen dynamically in such a way that the $(N+1)$-th term is smaller in absolute value than a user-defined cutoff relatively to the sum of the preceding N terms.

Eq. (15) factors out the non-perturbative part of the calculation represented by $f_{\rm NP}$ from the perturbative content. This is done on purpose to devise a method in which the perturbative content

[2]The superscript 0 in $z_n^{(0)}$ and $w_n^{(0)}$ indicates that here we are performing a Hankel tranform that involves the Bessel function of degree zero J_0. This is useful in view of the next section in which the integration over q_T will give rise to a similar Hankel transform with J_0 replaced by J_1. Also in that case the Ogata quadrature algorithm can be applied but coordinates and weights will be different.

is precomputed and numerically convoluted with the non-perturbative functions *a posteriori*. This is convenient in view of a fit of the function $f_{\rm NP}$.

As customary in QCD, the most convenient basis for the matching in Eq. (8) is the so-called "evolution" basis (*i.e.* Σ, V, T_3, V_3, etc.). In fact, in this basis the operator matrix C_{ij} is almost diagonal with the only exception of crossing terms that couple the gluon and the singlet Σ distributions. As a consequence, this is the most convenient basis for the computation of I_{ij}. On the other hand, TMDs in Eq. (1) appear in the so-called "physical" basis (*i.e.* d, $\bar{d}$, u, $\bar{u}$, etc.). Therefore, we need to rotate $F_{i(j)}$ from the evolution basis, over which the indices i and j run, to the physical basis. This is done by means of an appropriate constant matrix T, so that:

$$\overline{F}_q(x_1, b; \mu, \zeta) = \sum_i T_{qi} F_i(x_1, b; \mu, \zeta)\,, \tag{16}$$

and similarly for $\overline{F}_{\bar{q}}$. Putting all pieces together, one can conveniently write the cross section in Eq. (1) as:

$$\frac{d\sigma}{dQdydq_T} \simeq \sum_{n=1}^{N} w_n^{(0)} \frac{z_n^{(0)}}{q_T} S\left(x_1, x_2, \frac{z_n^{(0)}}{q_T}; \mu, \zeta\right) f_{\rm NP}\left(x_1, \frac{z_n^{(0)}}{q_T}, \zeta\right) f_{\rm NP}\left(x_2, \frac{z_n^{(0)}}{q_T}, \zeta\right)\,, \tag{17}$$

with:

$$S(x_1, x_2, b; \mu, \zeta) = \frac{8\pi\alpha^2}{9Q^3} H(Q, \mu) \sum_q C_q(Q) \left[\overline{F}_q\left(x_1, b_*(b); \mu, \zeta\right)\right] \left[\overline{F}_{\bar{q}}\left(x_2, b_*(b); \mu, \zeta\right)\right]\,. \tag{18}$$

Eq. (17) allows one to precompute the weights S in such a way that the differential cross section in Eq. (1) can be computed as a simple weighted sum of the non-perturbative contribution. A misleading aspect of Eq. (18) is the fact that S has five arguments. In actual facts, S only depends on three independent variables. The reason is that μ and ζ are usually taken to be proportional to Q by a constant factor. In addition x_1 and x_2 depend on Q and y through Eq. (2). Therefore, the full dependence on the kinematics of the final state of Eq. (1) can be specified by Q, y and q_T.

2 Integrating over the final-state kinematic variables

Despite Eq. (17) provides a powerful tool for a fast computation of cross sections, it is often not sufficient to allow for a direct comparison to experimental data. The reason is that experimental measurements of differential distributions are usually delivered as integrated over finite regions of the final-state kinematic phase space. In other words, experiments measure quantities like:

$$\widetilde{\sigma} = \int_{Q_{\rm min}}^{Q_{\rm max}} dQ \int_{y_{\rm min}}^{y_{\rm max}} dy \int_{q_{T,\rm min}}^{q_{T,\rm max}} dq_T \left[\frac{d\sigma}{dQdydq_T}\right]\,. \tag{19}$$

As a consequence, in order to guarantee performance, we need to include the integrations above in the precomputed factors.

2.1 Integrating over q_T

The integration over bins in q_T can be carried out analytically exploiting the following property of Bessel's function:

$$\frac{d}{dx}\left[x^m J_m(x)\right] = x^m J_{m-1}(x)\,, \tag{20}$$

that leads to:

$$\int dx\, x J_0(x) = x J_1(x) \quad \Rightarrow \quad \int_{x_1}^{x_2} dx\, x J_0(x) = x_2 J_1(x_2) - x_1 J_1(x_1)\,. \tag{21}$$

To see it, we observe that the differential cross section in Eq. (1) has the following structure:

$$\frac{d\sigma}{dQdydq_T} \propto \int_0^\infty db\, q_T J_0(bq_T)\dots \tag{22}$$

where the ellipses indicate terms that do not depend on q_T. Therefore, using Eq. (21) we find:

$$\begin{aligned}&\int_{q_{T,\min}}^{q_{T,\max}} dq_T \left[\frac{d\sigma}{dQdydq_T}\right] \propto \int_0^\infty db \int_{q_{T,\min}}^{q_{T,\max}} dq_T\, q_T J_0(bq_T)\cdots = \\ &\int_0^\infty \frac{db}{b^2} \int_{bq_{T,\min}}^{bq_{T,\max}} dx\, x J_0(x)\cdots = \int_0^\infty \frac{db}{b}\left[q_{T,\max}J_1(bq_{T,\max}) - q_{T,\min}J_1(bq_{T,\min})\right]\dots .\end{aligned} \tag{23}$$

Therefore, defining:

$$K(q_T) \equiv \int dq_T \left[\frac{d\sigma}{dQdydq_T}\right] \tag{24}$$

as the indefinite integral over q_T of the cross section in Eq. (1), we have that:

$$\int_{q_{T,\min}}^{q_{T,\max}} dq_T \left[\frac{d\sigma}{dQdydq_T}\right] = K(Q,y,q_{T,\max}) - K(Q,y,q_{T,\min})\,, \tag{25}$$

with:

$$\begin{aligned}K(Q,y,q_T) &= \frac{8\pi\alpha^2 q_T}{9Q^3} H(Q,\mu) \\ &\times \int_0^\infty db\, J_1(bq_T) \sum_q C_q(Q)\overline{F}_q(x_1,b;\mu,\zeta)\overline{F}_{\bar{q}}(x_2,b;\mu,\zeta) f_{\rm NP}(x_1,b,\zeta) f_{\rm NP}(x_2,b,\zeta)\,,\end{aligned} \tag{26}$$

that can be computed using the Ogata quadrature as:

$$K(Q,y,q_T) \simeq \sum_{n=1}^N w_n^{(1)} S\left(x_1, x_2, \frac{z_n^{(1)}}{q_T};\mu,\zeta\right) f_{\rm NP}\left(x_1, \frac{z_n^{(1)}}{q_T},\zeta\right) f_{\rm NP}\left(x_2, \frac{z_n^{(1)}}{q_T},\zeta\right)\,, \tag{27}$$

with S defined in Eq. (18). The unscaled coordinates $z_n^{(1)}$ and the weights $w_n^{(1)}$ can again be precomputed and stored in terms of the zero's of the Bessel function J_1. Eq. (25) reduces the integration in q_T to a calculation completely analogous to the unintegrated cross section. This is particularly convenient because it avoids the computation a numerical integration.

2.1.1 Kinematic cuts

In the presence of kinematic cuts, such as those on the final-state leptons in Drell-Yan, the analytic integration over q_T discussed above cannot be performed. The reason is that the implementation of these cuts effectively introduces a q_T-dependent function $\mathcal{P}$([3]) in the integral:

$$\frac{d\sigma}{dQdydq_T} \propto \int_0^\infty db\, q_T J_0(bq_T)\mathcal{P}(q_T)\dots\,, \tag{28}$$

that prevents the direct use of Eq. (21). Since $\mathcal{P}$ is a slowly-varying function of q_T over the typical bin size, we can approximate the integral over the bins in q_T as:

$$\begin{aligned}\int_{q_{T,\min}}^{q_{T,\max}} dq_T\, q_T J_0(bq_T)\mathcal{P}(q_T) &\simeq \mathcal{P}\left(\frac{q_{T,\max}+q_{T,\min}}{2}\right)\int_{q_{T,\min}}^{q_{T,\max}} dq_T\, q_T J_0(bq_T) \\ &= \mathcal{P}\left(\frac{q_{T,\max}+q_{T,\min}}{2}\right)\frac{1}{b}\left[q_{T,\max}J_1(bq_{T,\max}) - q_{T,\min}J_1(bq_{T,\min})\right]\,.\end{aligned} \tag{29}$$

[3] In fact, $\mathcal{P}$ also depends on the invariant mass Q and the rapidity y of the lepton pair that also need to be integrated over.

Unfortunately, this structure is inconvenient because it mixes different bin bounds and prevents a recursive computation. However, we can try to go further and, assuming that the bin width is small enough, we can expand $\mathcal{P}$ is the following ways:

$$\begin{aligned}
\mathcal{P}\left(\frac{q_{T,\max}+q_{T,\min}}{2}\right) &= \mathcal{P}\left(q_{T,\min}+\Delta q_T\right) = \mathcal{P}\left(q_{T,\min}\right) + \mathcal{P}'\left(q_{T,\min}\right)\Delta q_T + \mathcal{O}\left(\Delta q_T^2\right)\,, \\
\mathcal{P}\left(\frac{q_{T,\max}+q_{T,\min}}{2}\right) &= \mathcal{P}\left(q_{T,\max}-\Delta q_T\right) = \mathcal{P}\left(q_{T,\max}\right) - \mathcal{P}'\left(q_{T,\max}\right)\Delta q_T + \mathcal{O}\left(\Delta q_T^2\right)\,,
\end{aligned} \tag{30}$$

with:

$$\Delta q_T = \frac{q_{T,\max}-q_{T,\min}}{2}\,. \tag{31}$$

Therefore:

$$\begin{aligned}
b\int_{q_{T,\min}}^{q_{T,\max}} dq_T\, q_T J_0(bq_T)\mathcal{P}(q_T) \;&\simeq\; q_{T,\max}J_1(bq_{T,\max})\left[\mathcal{P}\left(q_{T,\max}\right) - \mathcal{P}'\left(q_{T,\max}\right)\Delta q_T\right] \\
&-\; q_{T,\min}J_1(bq_{T,\min})\left[\mathcal{P}\left(q_{T,\min}\right) + \mathcal{P}'\left(q_{T,\min}\right)\Delta q_T\right]\,.
\end{aligned} \tag{32}$$

The advantage of this formula as compared to Eq. (29) is that each single term depends on one single bin-bound in q_T rather than on a combination of two consecutive bounds. Therefore, in the presence of kinematic cuts, the actual form of the primitive function K defined in Eq. (25) and given explicitly in Eq. (26) is:

$$\begin{aligned}
K(Q,y,q_T) &= \frac{8\pi\alpha^2 q_T}{9Q^3}H(Q,\mu)\left[\mathcal{P}\left(Q,y,q_T\right) \pm \mathcal{P}'\left(Q,y,q_T\right)\Delta q_T\right] \\
&\times\int_0^\infty db\, J_1(bq_T)\sum_q C_q(Q)\overline{F}_q(x_1,b;\mu,\zeta)\overline{F}_{\bar{q}}(x_2,b;\mu,\zeta)f_{\rm NP}(x_1,b,\zeta)f_{\rm NP}(x_2,b,\zeta)\,,
\end{aligned} \tag{33}$$

where I have explicitly reinstated the dependence of the function $\mathcal{P}$ and its derivative with respect to q_T, $\mathcal{P}'$, on Q and y. In the square bracket in Eq. (33), the minus sign applies when q_T is the upper bound of the bin and the plus sign when it is the lower bound (see Eq. (32)). As discussed below, when integrating over bins in Q and y, one should also integrate the functions $\mathcal{P}$ and $\mathcal{P}'$. However, we will argue that, in the interpolation procedure discussed below, these functions can be extracted from the integrals in Q and y in a proper manner in such a way to avoid computing the expensive function $\mathcal{P}$ many times and, moreover, simplify enormously the structure of the resulting interpolation tables.

2.2 On the position of the peak of the q_T distribution

It is interesting at this point to take a short detour to discuss the position of the peak on the distribution in q_T of the cross section in Eq. (1). The peak can be located by setting the derivative in q_T of the cross section equal to zero. To do so, we use another property of Bessel's functions:

$$\frac{dJ_0(x)}{dx} = -J_1(x)\,. \tag{34}$$

Using this relation, it is easy to see that:

$$\begin{aligned}
0 &= \frac{d}{dq_T}\left[\frac{d\sigma}{dQdydq_T}\right] = \\
&\frac{8\pi\alpha^2}{9Q^3}H(Q,\mu)\int_0^\infty db\, b\left[J_0(bq_T) - bq_T J_1(bq_T)\right]\sum_q C_q(Q)\overline{F}_q(x_1,b_*(b);\mu,\zeta)\overline{F}_{\bar{q}}(x_2,b_*(b);\mu,\zeta) \\
&\times f_{\rm NP}(x_1,b,\zeta)f_{\rm NP}(x_2,b,\zeta)\,,
\end{aligned} \tag{35}$$

that is equivalent to require that:

$$\int_0^\infty db\, b\, [J_0(bq_T) - bq_T J_1(bq_T)] \sum_q C_q(Q)\overline{F}_q(x_1, b_*(b); \mu, \zeta)\overline{F}_{\bar{q}}(x_2, b_*(b); \mu, \zeta) f_{\rm NP}(x_1, b, \zeta) f_{\rm NP}(x_2, b, \zeta) = 0\,. \tag{36}$$

The integral above can be solved numerically using the technique discussed above and the value of q_T that satisfies this equation represents the position of the peak of the q_T distribution.

2.3 Integrating over Q and y

As a final step, we need to perform the integrals over Q and y defined in Eq. (19). To compute these integrals we can only rely on numerical methods. Having reduced the integration in q_T to the difference of the two terms in the r.h.s. of Eq. (25)([4]), we can concentrate on integrating the function K over Q and y for a fixed value of q_T:

$$\widetilde{K}(q_T) = \int_{Q_{\rm min}}^{Q_{\rm max}} dQ \int_{y_{\rm min}}^{y_{\rm max}} dy\, K(Q, y, q_T)\,, \tag{37}$$

such that:

$$\widetilde{\sigma} = \widetilde{K}(q_{T,\rm max}) - \widetilde{K}(q_{T,\rm min})\,. \tag{38}$$

To this purpose, it is convenient to make explicit the dependence of x_1 and x_2 on Q and y using Eq. (2). In addition, for the sake of simplicity we will identify the scales μ and $\sqrt{\zeta}$ with Q (possible scale variations can be easily reinstated at a later stage) and thus drop one of the arguments from the TMD distributions $\overline{F}$ and from the hard factor H. This yields:

$$\begin{aligned}
\widetilde{K}(q_T) &= \frac{8\pi q_T}{9} \int_0^\infty db\, J_1(bq_T) \int_{Q_{\rm min}}^{Q_{\rm max}} dQ \int_{e^{y_{\rm min}}}^{e^{y_{\rm max}}} \frac{d\xi}{\xi} \\
&\times \frac{1}{Q^3}\alpha^2(Q) H(Q) \sum_q C_q(Q)\overline{F}_q\left(\frac{Q}{\sqrt{s}}\xi, b_*(b); Q\right)\overline{F}_{\bar{q}}\left(\frac{Q}{\sqrt{s}}\frac{1}{\xi}, b_*(b); Q\right) \\
&\times f_{\rm NP}\left(\frac{Q}{\sqrt{s}}\xi, b; Q\right) f_{\rm NP}\left(\frac{Q}{\sqrt{s}}\frac{1}{\xi}, b; Q\right)\,,
\end{aligned} \tag{39}$$

where we have performed the change of variable $e^y = \xi$. Now we define one grid in ξ, $\{\xi_\alpha\}$ with $\alpha = 0, \ldots, N_\xi$, and one grid in Q, $\{Q_\tau\}$ with $\tau = 0, \ldots, N_Q$, each of which with a set of interpolating functions $\mathcal{I}$ associated. In addition, the grids are such that: $\xi_0 = e^{y_{\rm min}}$ and $\xi_{N_\xi} = e^{y_{\rm max}}$, and $Q_0 = Q_{\rm min}$ and $Q_{N_Q} = Q_{\rm max}$. More details on the interpolation procedure are presented in Appendix B. This allows us to interpolate the pair of functions $f_{\rm NP}$ in Eq. (39) for generic values of ξ and Q as:

$$f_{\rm NP}\left(\frac{Q}{\sqrt{s}}\xi, b; Q\right) f_{\rm NP}\left(\frac{Q}{\sqrt{s}}\frac{1}{\xi}, b; Q\right) \simeq \sum_{\alpha=0}^{N_\xi}\sum_{\tau=0}^{N_Q} \mathcal{I}_\alpha(\xi)\mathcal{I}_\tau(Q) f_{\rm NP}\left(\frac{Q_\tau}{\sqrt{s}}\xi_\alpha, b; Q_\tau\right) f_{\rm NP}\left(\frac{Q_\tau}{\sqrt{s}}\frac{1}{\xi_\alpha}, b; Q_\tau\right)\,. \tag{40}$$

Plugging the equation above into Eq. (39) we obtain:

$$\begin{aligned}
\widetilde{K}(q_T) &\simeq \frac{8\pi q_T}{9} \int_0^\infty db\, J_1(bq_T) \sum_{\tau=0}^{N_Q}\sum_{\alpha=0}^{N_\xi} \left[\int_{Q_{\rm min}}^{Q_{\rm max}} dQ\, \mathcal{I}_\tau(Q)\, \frac{1}{Q^3}\alpha^2(Q) H(Q)\right. \\
&\times \left.\int_{e^{y_{\rm min}}}^{e^{y_{\rm max}}} d\xi\, \mathcal{I}_\alpha(\xi)\, \frac{1}{\xi} \sum_q C_q(Q)\overline{F}_q\left(\frac{Q}{\sqrt{s}}\xi, b_*(b); Q\right)\overline{F}_{\bar{q}}\left(\frac{Q}{\sqrt{s}}\frac{1}{\xi}, b_*(b); Q\right)\right] \\
&\times f_{\rm NP}\left(\frac{Q_\tau}{\sqrt{s}}\xi_\alpha, b; Q_\tau\right) f_{\rm NP}\left(\frac{Q_\tau}{\sqrt{s}}\frac{1}{\xi_\alpha}, b; Q_\tau\right)\,.
\end{aligned} \tag{41}$$

[4] For the moment we ignore the complication introduced by the presence of cuts on the final state discussed in Sect. 2.1.1. We will come back on this issue at the end of the section.

Finally, the integration over b can be performed using the Ogata quadrature as discussed above, so that:

$$\begin{aligned}\widetilde{K}(q_T) &\simeq \sum_{n=1}^{N}\sum_{\tau=0}^{N_Q}\sum_{\alpha=0}^{N_\xi}\left[\frac{8\pi}{9}w_n^{(1)}\int_{Q_{\min}}^{Q_{\max}} dQ\,\mathcal{I}_\tau(Q)\,\frac{1}{Q^3}\alpha^2(Q)H(Q)\right.\\ &\times \left.\int_{e^{y_{\min}}}^{e^{y_{\max}}} d\xi\,\mathcal{I}_\alpha(\xi)\,\frac{1}{\xi}\sum_q C_q(Q)\overline{F}_q\left(\frac{Q}{\sqrt{s}}\xi, b_*\left(\frac{z_n}{q_T}\right);Q\right)\overline{F}_{\bar{q}}\left(\frac{Q}{\sqrt{s}}\frac{1}{\xi}, b_*\left(\frac{z_n}{q_T}\right);Q\right)\right] \qquad (42)\\ &\times f_{\rm NP}\left(\frac{Q_\tau}{\sqrt{s}}\xi_\alpha, \frac{z_n}{q_T}; Q_\tau\right) f_{\rm NP}\left(\frac{Q_\tau}{\sqrt{s}}\frac{1}{\xi_\alpha}, \frac{z_n}{q_T}; Q_\tau\right).\end{aligned}$$

In conclusion, if we define:

$$\begin{aligned}W_{n\tau\alpha}(q_T) &\equiv w_n^{(1)}\frac{8\pi}{9}\int_{Q_{\min}}^{Q_{\max}} dQ\,\mathcal{I}_\tau(Q)\,\frac{\alpha^2(Q)}{Q^3}H(Q)\\ &\times \int_{e^{y_{\min}}}^{e^{y_{\max}}} d\xi\,\mathcal{I}_\alpha(\xi)\,\frac{1}{\xi}\sum_q C_q(Q)\overline{F}_q\left(\frac{Q}{\sqrt{s}}\xi, b_*\left(\frac{z_n}{q_T}\right);Q\right)\overline{F}_{\bar{q}}\left(\frac{Q}{\sqrt{s}}\frac{1}{\xi}, b_*\left(\frac{z_n}{q_T}\right);Q\right),\end{aligned} \qquad (43)$$

the quantity $\widetilde{K}(q_T)$ can be computed as:

$$\widetilde{K}(q_T) \simeq \sum_{n=1}^{N}\sum_{\tau=0}^{N_Q}\sum_{\alpha=0}^{N_\xi} W_{n\tau\alpha}(q_T) f_{\rm NP}\left(\frac{Q_\tau}{\sqrt{s}}\xi_\alpha, \frac{z_n}{q_T}; Q_\tau\right) f_{\rm NP}\left(\frac{Q_\tau}{\sqrt{s}}\frac{1}{\xi_\alpha}, \frac{z_n}{q_T}; Q_\tau\right). \qquad (44)$$

The advantage of Eq. (44) is that the weights $W_{n\alpha\tau}$, that clearly depend on q_T but also on the intervals $[Q_{\min} : Q_{\max}]$ and $[y_{\min} : y_{\max}]$, can be precomputed once and for all for each of the experimental points included in a fit and used to determine the function $f_{\rm NP}$. This provides a fast tool for the computation of predictions that makes the extraction of the non-perturbative part of the TMDs much easier.

It is now time to discuss how the weights defined in Eq. (43) are affected by the presence of cuts as discussed in Sect. 2.1.1. In principle, the function between square brackets in Eq. (33) should be inside the integrals in Eq. (43) and integrated over the variable Q and $\xi = e^y$. However, this turns out to be numerically problematic because the phase-space-reduction function $\mathcal{P}$ is expensive to compute. On top of this, the fact that the factor between square brackets in Eq. (33) depends on whether q_T is a lower or an upper integration bound would lead to a duplication of the weights to compute. In order to simplify the computation, we assume that the function $\mathcal{P}$ and its derivative $\mathcal{P}'$ are slowly varying functions of Q and y over the typical grid interval of the grids in Q and ξ. In addition, the interpolating functions $\mathcal{I}_\tau(Q)$ and $\mathcal{I}_\alpha(\xi)$ are strongly peaked at Q_τ and ξ_α, respectively. These considerations allow us to avoid integrating explicitly $\mathcal{P}$ and $\mathcal{P}'$ over Q and ξ and to replace the weights in Eq. (43) with:

$$W_{n\tau\alpha}(q_T) \to \left[\mathcal{P}\left(Q_\tau, \ln(\xi_\alpha), q_T\right) \pm \mathcal{P}'\left(Q_\tau, \ln(\xi_\alpha), q_T\right)\Delta q_T\right] W_{n\tau\alpha}(q_T). \qquad (45)$$

At the end of the day, the only additional information required to implement cuts on the final state is the value of the phase-space-reduction function $\mathcal{P}$ and its derivative $\mathcal{P}'$ on all points of the bidimensional grid in Q and ξ for all q_T bin bounds. Eq. (45) will then allow one to use the weights computed over the full phase space. We will check the accuracy of this procedure by comparing it to the explicit integration.

2.4 Cross section differential in x_F

In some cases, the Drell-Yan differential cross section may be presented as differential in the invariant mass of the lepton pair Q and, instead of the rapidity y, of the Feynman variable x_F defined as:

$$x_F = \frac{Q}{\sqrt{s}}\left(e^y - e^{-y}\right) = \frac{2Q}{\sqrt{s}}\sinh y = x_1 - x_2\,, \tag{46}$$

so that:

$$\frac{dx_F}{dy} = \frac{2Q}{\sqrt{s}}\cosh y = x_1 + x_2\,. \tag{47}$$

Therefore:

$$\frac{d\sigma}{dQdx_Fdq_T} = \frac{dy}{dx_F}\frac{d\sigma}{dQdydq_T} = \frac{\sqrt{s}}{2Q\cosh y}\frac{d\sigma}{dQdydq_T} = \frac{1}{x_1+x_2}\frac{d\sigma}{dQdydq_T} \tag{48}$$

with:

$$y(x_F,Q) = \sinh^{-1}\left(\frac{x_F\sqrt{s}}{2Q}\right) = \ln\left[\frac{\sqrt{s}}{2Q}\left(x_F + \sqrt{x_F^2 + \frac{4Q^2}{s}}\right)\right]\,, \tag{49}$$

so that:

$$x_1 = \frac{1}{2}\left(x_F + \sqrt{x_F^2 + \frac{4Q^2}{s}}\right) \quad \text{and} \quad x_2 = \frac{Q^2}{sx_1}\,. \tag{50}$$

Therefore, we can compute the integral:

$$\widetilde{I}(q_T) = \int_{Q_{\min}}^{Q_{\max}} dQ \int_{x_{F,\min}}^{x_{F,\max}} dx_F\, I(Q,x_F,q_T)\,, \tag{51}$$

where I is the primitive in q_T of the cross section differential in x_F:

$$I(Q,x_F,q_T) = \int dq_T \left[\frac{d\sigma}{dQdx_Fdq_T}\right]\,, \tag{52}$$

following the same steps of Sect. 2.3. This leads to:

$$\widetilde{I}(q_T) \;\simeq\; \sum_{n=1}^{N}\sum_{\tau=0}^{N_Q}\sum_{\alpha=0}^{N_x} \overline{W}_{n\tau\alpha}(q_T) f_{\rm NP}\left(x_{1,\alpha\tau}, \frac{z_n}{q_T}; Q_\tau\right) f_{\rm NP}\left(x_{2,\alpha\tau}, \frac{z_n}{q_T}; Q_\tau\right)\,, \tag{53}$$

with:

$$\begin{aligned}\overline{W}_{n\tau\alpha}(q_T) \;\equiv\; & w_n^{(1)}\frac{8\pi}{9}\int_{Q_{\min}}^{Q_{\max}} dQ\, \mathcal{I}_\tau(Q)\,\frac{1}{Q^3}\alpha^2(Q)H(Q) \\ \times\; & \int_{x_{F,\min}}^{x_{F,\max}} dx_F\, \mathcal{I}_\alpha(x_F)\,\frac{1}{x_1+x_2}\sum_q C_q(Q)\overline{F}_q\left(x_1, b_*\left(\frac{z_n}{q_T}\right); Q\right)\overline{F}_{\bar{q}}\left(x_2, b_*\left(\frac{z_n}{q_T}\right); Q\right)\,,\end{aligned} \tag{54}$$

where x_1 and x_2 are functions of x_F and Q through Eq. (50). In addition, we have defined a grid in x_F, $\{x_{F,\alpha}\}$ with $\alpha = 0,\ldots,N_x$, that allowed us to define $x_{1(2),\alpha\tau} \equiv x_{1(2)}(x_{F,\alpha}, Q_\tau)$.

2.5 Flavour dependence

It may be advantageous to introduce a flavour dependence of the non-perturbative contributions to TMDs. This can be easily done by observing that the tensor $W_{n\tau\alpha}$ defined in Eq. (43) can be decomposed as[5]:

$$W_{n\tau\alpha}(q_T) = \sum_q W^{(q)}_{n\tau\alpha}(q_T)\,, \tag{55}$$

[5]The same procedure applies to the tensor $\overline{W}_{n\tau\alpha}$ defined in Eq. (54).

with:

$$\begin{aligned} W^{(q)}_{n\tau\alpha}(q_T) &\equiv w^{(1)}_n \frac{8\pi}{9} \int_{Q_{\min}}^{Q_{\max}} dQ\, \mathcal{I}_\tau(Q)\, \frac{\alpha^2(Q)}{Q^3} H(Q) C_q(Q) \\ &\times \int_{e^{y_{\min}}}^{e^{y_{\max}}} d\xi\, \mathcal{I}_\alpha(\xi)\, \frac{1}{\xi} \overline{F}_q\left(\frac{Q}{\sqrt{s}}\xi, b_*\left(\frac{z_n}{q_T}\right); Q\right) \overline{F}_{\bar{q}}\left(\frac{Q}{\sqrt{s}}\frac{1}{\xi}, b_*\left(\frac{z_n}{q_T}\right); Q\right) . \end{aligned} \tag{56}$$

This allows for an independent parameterisation of the non-perturbative contribution such that Eq. (44) can be written as:

$$\widetilde{K}(q_T) \simeq \sum_q \sum_{n=1}^{N} \sum_{\tau=0}^{N_Q} \sum_{\alpha=0}^{N_\xi} W^{(q)}_{n\tau\alpha}(q_T) f^{(q)}_{\rm NP}\left(\frac{Q_\tau}{\sqrt{s}}\xi_\alpha, \frac{z_n}{q_T}; Q_\tau\right) f^{(q)}_{\rm NP}\left(\frac{Q_\tau}{\sqrt{s}}\frac{1}{\xi_\alpha}, \frac{z_n}{q_T}; Q_\tau\right) , \tag{57}$$

where $f^{(q)}_{\rm NP}$ parametrises the non-perturbative component of the TMD with flavour q.

2.6 Gradient with respect to the free parameters

A very appealing implication of the computation of cross section in terms of precomputed table as in Eqs. (44) and (57) is the fact that it exposes the free parameters of the non-perturbative functions. To be more specific, the non-perturbative function $f_{\rm NP}$, on top of being a function of x, b, and ζ, depends parameterically on a set of N_p parameters $\{\theta_k\}$, $k = 1, \ldots, N_p$, that are typically determined by fits to data, in other words:

$$f_{\rm NP} \equiv f_{\rm NP}\left(x, b, \zeta; \{\theta_k\}\right) . \tag{58}$$

Now, when performing a fit, it is very useful to be able to compute the derivative of the figure of merit (usually the χ^2) with respect to the parameters to be determined. In turn, this immediately implies being able to compute the derivative of the observables. Referring to Eq. (44), the relevant quantity is:

$$\frac{d\widetilde{K}}{d\theta_k} = \sum_{n=1}^{N} \sum_{\tau=0}^{N_Q} \sum_{\alpha=0}^{N_\xi} W_{n\tau\alpha}(q_T) \left[\frac{df^{(1)}_{\rm NP}}{d\theta_k} f^{(2)}_{\rm NP} + f^{(1)}_{\rm NP} \frac{df^{(2)}_{\rm NP}}{d\theta_k}\right] , \tag{59}$$

where $f^{(1)}_{\rm NP}$ and $f^{(2)}_{\rm NP}$ refer to the non-perturbative function $f_{\rm NP}$ computed in x_1 and x_2, respectively. It is thus clear that the derivatives w.r.t. the free parameters penetrates the observable. Since in most cases the derivative of $f_{\rm NP}$ can be computed analytically, this allows one to compute the gradient of the figure of merit analytically. This potentially makes any fit much simpler.

2.7 Narrow-width approximation

A possible alternative to the numerical integration in Q when the integration region includes the Z-peak region is the so-called narrow-width approximation (NWA). In the NWA one assumes that the width of the Z boson, Γ_Z, is much smaller than its mass, M_Z. This way one can approximate the peaked behaviour of the couplings $C_q(Q)$ around $Q = M_Z$ with a δ-function, *i.e.* $C_q(Q) \sim \delta(Q^2 - M_Z^2)$. Therefore, the integration over Q can be done analytically. The exact structure of the electroweak couplings is the following:

$$C_q(Q) = e_q^2 - 2e_q V_q V_e \chi_1(Q) + (V_e^2 + A_e^2)(V_q^2 + A_q^2)\chi_2(Q) , \tag{60}$$

with:

$$\begin{aligned} \chi_1(Q) &= \frac{1}{4\sin^2\theta_W \cos^2\theta_W} \frac{Q^2(Q^2 - M_Z^2)}{(Q^2 - M_Z^2)^2 + M_Z^2\Gamma_Z^2} , \\ \chi_2(Q) &= \frac{1}{16\sin^4\theta_W \cos^4\theta_W} \frac{Q^4}{(Q^2 - M_Z^2)^2 + M_Z^2\Gamma_Z^2} . \end{aligned} \tag{61}$$

In the limit $\Gamma_Z/M_Z \to 0$, the leading contribution to the coupling in Eq. (60) comes from the region $Q \simeq M_Z$ and is that proportional to χ_2:

$$C_q(Q) \simeq (V_e^2 + A_e^2)(V_q^2 + A_q^2)\chi_2(Q)\,, \quad Q \simeq M_Z\,. \tag{62}$$

In addition, in this limit one can show that:

$$\frac{1}{(Q^2 - M_Z^2)^2 + M_Z^2\Gamma_Z^2} \to \frac{\pi}{M_Z\Gamma_Z}\delta(Q^2 - M_Z^2) = \frac{\pi}{2M_Z^2\Gamma_Z}\delta(Q - M_Z)\,. \tag{63}$$

Therefore, considering that:

$$\Gamma_Z = \frac{\alpha M_Z}{\sin^2\theta_W \cos^2\theta_W}\,, \tag{64}$$

the electroweak couplings in the NWA have the following form:

$$C_q(Q) \simeq \frac{\pi M_Z(V_e^2 + A_e^2)(V_q^2 + A_q^2)}{32\alpha \sin^2\theta_W \cos^2\theta_W}\delta(Q - M_Z) = \widetilde{C}_q(Q)\delta(Q - M_Z)\,. \tag{65}$$

Therefore, using Eq. (65) the integral of the cross section over Q under the condition that $Q_{\min} < M_Z < Q_{\max}$ has the consequence of adjusting the couplings and of setting $Q = M_Z$ in the computation. This yields:

$$\int_{Q_{\min}}^{Q_{\max}} dQ\,\frac{d\sigma}{dQdyd q_T} = \frac{16\pi\alpha^2 q_T}{9M_Z^3}H(M_Z, M_Z)\sum_q \widetilde{C}_q(M_Z)I_{q\bar{q}}(x_1, x_2, q_T; M_Z, M_Z^2)\,, \tag{66}$$

where we are also assuming that $\mu = \sqrt{\zeta} = M_Z$. As a final step, one may want to let the Z boson decay into leptons. At leading order in the EW sector and assuming an equal decay rate for electrons, muons, and tauons, this can be done by multiplying the cross section above by three times the branching ratio for the Z decaying into any pair of leptons, $3\mathrm{Br}(Z \to \ell^+\ell^-)$.

A Ogata quadrature

In this section we limit ourselves to write the formulas for the computation of the unscaled coordinates $z_n^{(\nu)}$ and weights $w_n^{(\nu)}$ required to compute the following integral:

$$I_\nu(q_T) = \int_0^\infty dbJ_\nu(bq_T)f\,(b) = \frac{1}{q_T}\int_0^\infty d\bar{b}J_\nu(\bar{b})f\left(\frac{\bar{b}}{q_T}\right) \simeq \frac{1}{q_T}\sum_{n=1}^\infty w_n^{(\nu)} f\left(\frac{z_n^{(\nu)}}{q_T}\right) \quad \nu = 0, 1, \dots\,, \tag{67}$$

using the Ogata-quadrature algorithm. More details can be found in Ref. [3]. There relevant formulas are:

$$\begin{aligned} z_n^{(\nu)} &= \frac{\pi}{h}\psi\left(\frac{h\xi_{\nu n}}{\pi}\right)\,, \\ w_n^{(\nu)} &= \pi\frac{Y_\nu(\xi_{\nu n})}{J_{\nu+1}(\xi_{\nu n})}J_\nu(z_n^{(\nu)})\psi'\left(\frac{h\xi_{\nu n}}{\pi}\right)\,. \end{aligned} \tag{68}$$

where:

- h is a free parameter of the algorithm that has to be typically small (we choose $h = 10^{-3}$),
- $\xi_{\nu n}$ are the zero's of J_ν, *i.e.* $J_\nu(\xi_{\nu n}) = 0\ \forall\, n$,
- J_ν and Y_ν are the Bessel functions of first and second kind, respectively, of degree ν,
- ψ is the following function:

$$\psi(t) = t\tanh\left(\frac{\pi}{2}\sinh t\right) \tag{69}$$

and its derivative:

$$\psi'(t) = \frac{\pi t\cosh t + \sinh(\pi\sinh t)}{1 + \cosh(\pi\sinh t)}\,. \tag{70}$$

B Lagrange interpolation

Just for the record, it is useful to derive a general expression for the Lagrange interpolating functions $\mathcal{I}$ introduced in Eq. (40) and used to interpolate the non-perturbative functions $f_{\rm NP}$. More, importantly, we need to understand how these functions behave upon integration.

Suppose one wants to interpolate the test function g in the point x using a set of Lagrange polynomials of degree k of. This requires a subset of $k+1$ consecutive points on an interpolation grid, say $\{x_\alpha, \ldots, x_{\alpha+k}\}$. The relative position between the point x and the subset of points used for the interpolation is arbitrary. It is convenient to choose the subset of points such that $x_\alpha < x \leq x_{\alpha+k}$.[6] However, the ambiguity remains because there are k possible choices according to whether $x_\alpha < x \leq x_{\alpha+1}$, or $x_{\alpha+1} < x \leq x_{\alpha+2}$, and so on.

In order to determine the exact form of the interpolation functions $\mathcal{I}$, let us see how to derive eq. (40). Using the standard Lagrange interpolation procedure, we can approximate the function g in x as:

$$g(x) = \sum_{i=0}^{k} \ell_i^{(k)}(x) g(x_{\alpha+i}) \,, \tag{71}$$

where $\ell_i^{(k)}$ is the i-th Lagrange polynomial of degree k which can be written as:

$$\ell_i^{(k)}(x) = \prod_{m=0, m\neq i}^{k} \frac{x - x_{\alpha+m}}{x_{\alpha+i} - x_{\alpha+m}} \,. \tag{72}$$

We now assume that:

$$x_\alpha < x \leq x_{\alpha+1} \,, \tag{73}$$

Eq. (71) becomes:

$$g(x) = \theta(x - x_\alpha)\theta(x_{\alpha+1} - x) \sum_{i=0}^{k} g(x_{\alpha+i}) \prod_{m=0, m\neq i}^{k} \frac{x - x_{\alpha+m}}{x_{\alpha+i} - x_{\alpha+m}} \,. \tag{74}$$

In order to make Eq. (74) valid for all values of α, one just has to sum over all N_x intervals of the *global* interpolation grid $\{x_0, \ldots, x_{N_x}\}$, that is:

$$g(x) = \sum_{\alpha=0}^{N_x-1} \theta(x - x_\alpha)\theta(x_{\alpha+1} - x) \sum_{i=0}^{k} g(x_{\alpha+i}) \prod_{m=0, m\neq i}^{k} \frac{x - x_{\alpha+m}}{x_{\alpha+i} - x_{\alpha+m}} \,, \tag{75}$$

Defining $\beta = \alpha + i$, we can rearrange the equation above as:

$$g(x) = \sum_{\beta=0}^{N_x+k-1} \mathcal{I}_\beta^{(k)}(x) g(x_\beta) \,, \tag{76}$$

that leads us to the definition of the interpolating functions:

$$\mathcal{I}_\beta^{(k)}(x) = \sum_{i=0, i\leq\beta}^{k} \theta(x - x_{\beta-i})\theta(x_{\beta-i+1} - x) \prod_{m=0, m\neq i}^{k} \frac{x - x_{\beta-i+m}}{x_\beta - x_{\beta-i+m}} \,, \tag{77}$$

where the condition $i \leq \beta$ comes from the condition $\alpha \geq 0$. It is important to observe that the sum in Eq. (76) extends up to the $(N_x + k - 1)$-th node. Therefore, the original grid needs to be extended by $k - 1$ nodes. However, the range of validity of the interpolation remains that defined by the original

[6] In fact, it is not even necessary to impose the constraint $x_\alpha < x \leq x_{\alpha+k}$. In case this relation is not fulfilled one usually refers to *extrapolation* rather than *interpolation*. If not necessary, this option is typically not convenient because it may lead to a substantial deterioration in the accuracy with which $g(x)$ is determined.

grid, *i.e.* $x_0 \leq x \leq x_{N_x}$. Finally, it is crucial to realise that the interpolation function $\mathcal{I}_\beta^{(k)}(x)$ is different from zero only over a limited interval, specifically:

$$\mathcal{I}_\beta^{(k)}(x) \neq 0 \quad \Leftrightarrow \quad x_{\beta-k} < x < x_{\beta+1}\,. \tag{78}$$

In the rest of this document we will stick to the assumption in Eq. (73). However, before going further, it is interesting to generalise Eq. (73) to:

$$x_{\alpha+t} < x \leq x_{\alpha+t+1} \quad \text{with} \quad t = 0, \ldots, k-1\,, \tag{79}$$

such that the interpolation formula becomes:

$$g(x) = \sum_{\alpha=-t}^{N_x-t-1} \theta(x - x_{\alpha+t})\theta(x_{\alpha+t+1} - x) \sum_{i=0}^{k} g(x_{\alpha+i}) \prod_{m=0, m\neq i}^{k} \frac{x - x_{\alpha+m}}{x_{\alpha+i} - x_{\alpha+m}}\,, \tag{80}$$

that can be rearranged as:

$$g(x) = \sum_{\beta=-t}^{N_x+k-t-1} \mathcal{I}_{\beta,t}^{(k)}(x) g(x_\beta)\,, \tag{81}$$

with:

$$\mathcal{I}_{\beta,t}^{(k)}(x) = \sum_{i=0, i\leq\beta}^{k} \theta(x - x_{\beta-i+t})\theta(x_{\beta-i+t+1} - x) \prod_{m=0, m\neq i}^{k} \frac{x - x_{\beta-i+m}}{x_\beta - x_{\beta-i+m}}\,, \tag{82}$$

being the "generalised" interpolation functions. The generalised interpolation functions can be used to overcome the "drawback" of requiring $k-1$ additional nodes on the interpolation grid. In practice, given the grid $\{x_0, \ldots, x_{N_x}\}$, one can tune t according to the position of x on the grid. More specifically, one can choose t in such a way that $\beta + t$ in Eq. (82) never exceeds N_x.

Now suppose we want to compute the following intergral:

$$I_1 = \int_{x_0}^{x_{N_x}} dx\, g(x) f(x)\,, \tag{83}$$

where f is some other function that we don't want to interpolate. Using Eqs. (76) and (78) we finally have that:

$$I_1 = \sum_{\beta=0}^{N_x+k-1} W_\beta g(x_\beta)\,, \tag{84}$$

with:

$$W_\beta = \int_{x_{\max(0,\beta-k)}}^{x_{\min(N_x,\beta+1)}} dx\, \mathcal{I}_\beta^{(k)}(x) f(x)\,. \tag{85}$$

The equation above can be easily generalised to a bidimensional integral as:

$$I_2 = \int_{x_0}^{x_{N_x}} dx \int_{y_0}^{y_{N_y}} dy\, g(x,y) f(x,y) = \sum_{\alpha=0}^{N_x+k-1} \sum_{\beta=0}^{N_y+l-1} W_{\alpha\beta} g(x_\alpha, y_\beta)\,, \tag{86}$$

with:

$$W_{\alpha\beta} = \int_{x_{\max(0,\alpha-k)}}^{x_{\min(N_x,\alpha+1)}} dx \int_{y_{\max(0,\beta-k)}}^{y_{\min(N_y,\beta+1)}} dy\, \mathcal{I}_\alpha^{(k)}(x)\, \mathcal{I}_\beta^{(l)}(y)\, f(x,y)\,. \tag{87}$$

This formalism nicely applies to the integral in Q and $\xi = e^y$ discussed above in Eq. (43). In view of a numerical implementation, it is worth noticing that the functions $\mathcal{I}$ are piecewise. In particular, while these functions are continuos in correspondence of the nodes of the grid, their first derivative is not. As a consequence, the result of the numerical integrals in Eqs. (85) and (87) may be inaccurate. To overcome this problem, it is sufficient to split the integrals in sub-integrals over the intervals delimited by two consecutive nodes. Using Eq. (78), it is easy to see that, for an interpolation of degree k, one needs to do $k+1$ integrals over the intervals included between the $(\beta-k)$-th and the $(\beta+1)$-th node.

C Cuts on the final-state leptons

In this section we derive explicitly the phase-space reduction factor $\mathcal{P}$ introduced in Sect. 2.1.1. This factor is defined as:

$$\mathcal{P}(Q,y,q_T) = \mathcal{P}(q) = \frac{\displaystyle\int_{\text{fid. reg.}} d^4p_1 d^4p_2\, \delta(p_1^2)\delta(p_2^2)\theta(p_{1,0})\theta(p_{2,0})\delta^{(4)}(p_1+p_2-q) g_{\mu\nu}L^{\mu\nu}(p_1,p_2)}{\displaystyle\int d^4p_1 d^4p_2\, \delta(p_1^2)\delta(p_2^2)\theta(p_{1,0})\theta(p_{2,0})\delta^{(4)}(p_1+p_2-q) g_{\mu\nu}L^{\mu\nu}(p_1,p_2)}\,, \tag{88}$$

where p_1 and p_2 are the four-momenta of the outgoing leptons and $L^{\mu\nu}$ is the leptonic tensor that, assuming massless leptons, reads:

$$L^{\mu\nu}(p_1,p_2) = 4(p_1^\mu p_2^\nu + p_2^\mu p_1^\nu - g^{\mu\nu}p_1p_2)\,, \tag{89}$$

so that:

$$g_{\mu\nu}L^{\mu\nu}(p_1,p_2) = -8(p_1p_2) = -4(p_1+p_2)^2\,. \tag{90}$$

In the last step we have used the on-shell-ness of the leptons ($p_1^2 = p_2^2 = 0$). The integral in the denominator of Eq. (88) is restricted to some *fiducial region*. Finally, we find:

$$\mathcal{P}(q) = \frac{\displaystyle\int_{\text{fid. reg.}} d^4p_1 d^4p_2\, \delta(p_1^2)\delta(p_2^2)\theta(p_{1,0})\theta(p_{2,0})\delta^{(4)}(p_1+p_2-q)(p_1+p_2)^2}{\displaystyle\int d^4p_1 d^4p_2\, \delta(p_1^2)\delta(p_2^2)\theta(p_{1,0})\theta(p_{2,0})\delta^{(4)}(p_1+p_2-q)(p_1+p_2)^2}\,. \tag{91}$$

The effect of integrating over the fiducial region can be implemented by defining a generalised θ-function, $\Phi(p_1,p_2)$, that is equal to one inside the fiducial region and zero outside. This allows one to integrate also the numerator of Eq. (91) over the full phase-space of the two outgoing leptons:

$$\mathcal{P}(q) = \frac{\displaystyle\int d^4p_1 d^4p_2\, \delta(p_1^2)\delta(p_2^2)\theta(p_{1,0})\theta(p_{2,0})\delta^{(4)}(p_1+p_2-q)\Phi(p_1,p_2)(p_1+p_2)^2}{\displaystyle\int d^4p_1 d^4p_2\, \delta(p_1^2)\delta(p_2^2)\theta(p_{1,0})\theta(p_{2,0})\delta^{(4)}(p_1+p_2-q)(p_1+p_2)^2}\,. \tag{92}$$

Now we can integrate over one of the outgoing momenta, say p_2, exploiting the momentum-conservation δ-function both in the numerator and in the denominator. Specifically, the numerator of Eq. (92) gives:

$$\begin{aligned}&\int d^4p_1 d^4p_2\, \delta(p_1^2)\delta(p_2^2)\theta(p_{1,0})\theta(p_{2,0})\delta^{(4)}(p_1+p_2-q)\Phi(p_1,p_2)(p_1+p_2)^2 = \\ &\qquad Q^2\int d^4p_1\,\delta(p_1^2)\delta((q-p_1)^2)\theta(p_{1,0})\theta(q_0-p_{1,0})\Phi(p_1,q-p_1)\,,\end{aligned} \tag{93}$$

and likewise in the denominator setting $\Phi(p_1,p_2)=1$. Finally, renaming $p_1 = p$, the phase-space reduction factor reads:

$$\mathcal{P}(q) = \frac{\displaystyle\int d^4p\,\delta(p^2)\delta((q-p)^2)\theta(p_0)\theta(q_0-p_0)\Phi(p,q-p)}{\displaystyle\int d^4p\,\delta(p^2)\delta((q-p)^2)\theta(p_0)\theta(q_0-p_0)}\,. \tag{94}$$

The δ-functions can now be used to constrain two of the four components of the momentum p. The first, $\delta(p_2^2)$, is usually used to set the first component of p, the energy, to the on-shell value. Since the leptons are assumed to be massless, this produces:

$$\int d^4p\,\delta(p^2)\theta(p_0) = \int d^4p\,\delta(E^2-|\mathbf{p}|^2)\theta(E) = \int \frac{dEd^3\mathbf{p}}{2|\mathbf{p}|}\delta(E-|\mathbf{p}|) = \int\frac{d^3\mathbf{p}}{2|\mathbf{p}|}\,. \tag{95}$$

Of course, the four-momentum p appearing in the rest of the integrand has to be set on shell ($E = |\mathbf{p}|$). Now we express the three-dimensional measure $d^3\mathbf{p}$ in spherical coordinates as:

$$d^3\mathbf{p} = |\mathbf{p}|^2 d|\mathbf{p}| d(\cos\theta) d\phi \,. \tag{96}$$

Then we make a change of variable from $(|\mathbf{p}|, \cos\theta)$ to $(|\mathbf{p}_T|, \eta)$: the second set of variables are exactly those on which kinematic cuts are imposed. We do so by knowing that:

$$\begin{cases} |\mathbf{p}| = |\mathbf{p}_T| \cosh\eta \,, \\ \cos\theta = \tanh\eta \,. \end{cases} \tag{97}$$

This leads to:

$$\int \frac{d^3\mathbf{p}}{2|\mathbf{p}|} = \frac{1}{2}\int |\mathbf{p}| d|\mathbf{p}| d(\cos\theta) d\phi = \frac{1}{2}\int |\mathbf{p}_T| d|\mathbf{p}_T| d\eta d\phi = \frac{1}{2}\int d^2\mathbf{p}_T d\eta \,. \tag{98}$$

Now we consider the second δ-function:

$$\frac{1}{2}\int d^2\mathbf{p}_T d\eta\, \delta((q-p)^2)\theta(q_0 - p_0) = \frac{1}{2}\int_{-\infty}^{\infty} d\eta \int_0^{2\pi} d\phi \int_0^{\infty} |\mathbf{p}_T| d|\mathbf{p}_T|\, \delta(Q^2 - 2p\cdot q)\theta(q_0 - p_0) \,, \tag{99}$$

being $q^2 = Q^2$ and $p^2 = 0$. It is convenient to express the four-vector q in terms of Q, y, and $\mathbf{q}_T$:

$$q = (M\cosh y, \mathbf{q}_T, M\sinh y) \,. \tag{100}$$

with $M = \sqrt{Q^2 + |\mathbf{q}_T|^2}$. While:

$$p = (|\mathbf{p}_T|\cosh\eta, \mathbf{p}_T, |\mathbf{p}_T|\sinh\eta) \,, \tag{101}$$

so that:

$$p\cdot q = |\mathbf{p}_T| M\left(\cosh\eta\cosh y - \sinh\eta\sinh y\right) - \mathbf{p}_T\cdot\mathbf{q}_T = |\mathbf{p}_T| M\cosh(\eta - y) - \mathbf{p}_T\cdot\mathbf{q}_T \,. \tag{102}$$

We can now assume that the two-dimensional vector $\mathbf{q}_T$ is aligned with the x axis so that $\mathbf{p}_T\cdot\mathbf{q}_T = |\mathbf{p}_T||\mathbf{q}_T|\cos\phi$([7]). Therefore, the argument of the δ-function in Eq. (99) becomes:

$$f(|\mathbf{p}_T|, \eta, \phi) = Q^2 - 2|\mathbf{p}_T|\left[M\cosh(\eta - y) - |\mathbf{q}_T|\cos\phi\right] \,. \tag{103}$$

and that of the ϑ-function $M\cosh y - |\mathbf{p}_T|\cosh\eta$. It thus appears convenient to integrate Eq. (99) over $|\mathbf{p}_T|$ first:

$$\frac{1}{2}\int_0^{\infty} |\mathbf{p}_T| d|\mathbf{p}_T|\, \delta(Q^2 - 2p\cdot q)\theta(q_0 - p_0) = \frac{\overline{p}_T^2}{2Q^2}\vartheta(M\cosh y - \overline{p}_T\cosh\eta) = \frac{\overline{p}_T^2}{2Q^2} \,, \tag{104}$$

with([8]):

$$\overline{p}_T(\cos\phi) = \frac{Q^2}{2\left[M\cosh(\eta - y) - |\mathbf{q}_T|\cos\phi\right]} = \frac{Q^2}{2|\mathbf{q}_T|}\frac{1}{\left[\frac{M\cosh(\eta-y)}{|\mathbf{q}_T|} - \cos\phi\right]} \,. \tag{105}$$

Now we turn to consider the integral in $d\phi$. To this end, the following relations are useful:

$$\int_0^{2\pi} d\phi\, f(\cos\phi) = \int_{-1}^{1} \frac{dx}{\sqrt{1-x^2}}\left[f(x) + f(-x)\right] \,. \tag{106}$$

and:

$$\int \frac{dx}{(a\pm x)^2\sqrt{1-x^2}} = \frac{\sqrt{1-x^2}}{(a^2-1)(x\pm a)} \pm \frac{a}{(a^2-1)^{3/2}}\tan^{-1}\left(\frac{1\pm ax}{\sqrt{a^2-1}\sqrt{1-x^2}}\right) \,. \tag{107}$$

[7] In the general case in which $\mathbf{q}_T$ forms an angle β with the x axis, the scalar product would result in $|\mathbf{p}_T||\mathbf{q}_T|\cos(\phi - \beta)$. However, the angle β could always be reabsorbed in a redefinition of the integration angle ϕ in Eq. (99).

[8] Notice that the ϑ-function has no effect. I have verified it numerically but I cannot see it analytically.

The last integral is such that:

$$\int_{-1}^{1} \frac{dx}{(a \pm x)^2 \sqrt{1-x^2}} = \frac{\pi a}{(a^2-1)^{3/2}} \,. \tag{108}$$

We now use Eqs. (106)-(108) to compute:

$$\begin{aligned}
&\frac{1}{2Q^2}\int_0^{2\pi} d\phi \, [\overline{p}_T(\cos\phi)]^2 = \frac{Q^2}{4|\mathbf{q}_T|^2}\int_0^{2\pi} \frac{d\phi}{\left[\frac{M\cosh(\eta-y)}{|\mathbf{q}_T|} - \cos\phi\right]^2} \\
&= \frac{Q^2}{8|\mathbf{q}_T|^2}\int_{-1}^{1}\frac{dx}{\sqrt{1-x^2}}\left[\frac{1}{\left(\frac{M\cosh(\eta-y)}{|\mathbf{q}_T|}-x\right)^2} + \frac{1}{\left(\frac{M\cosh(\eta-y)}{|\mathbf{q}_T|}+x\right)^2}\right] \\
&= \frac{Q^2}{8}\left\{\frac{|\mathbf{q}_T|^2 x\sqrt{1-x^2}}{(M^2\cosh^2(\eta-y)-|\mathbf{q}_T|^2)(x^2|\mathbf{q}_T|^2 - M^2\cosh^2(\eta-y))}\right. \\
&- \frac{M\cosh(\eta-y)}{(M^2\cosh^2(\eta-y)-|\mathbf{q}_T|^2)^{3/2}}\left[\tan^{-1}\left(\frac{|\mathbf{q}_T| - xM\cosh(\eta-y)}{\sqrt{(M^2\cosh^2(\eta-y)-|\mathbf{q}_T|^2)}\sqrt{1-x^2}}\right)\right. \\
&\left.\left. - \tan^{-1}\left(\frac{|\mathbf{q}_T| + xM\cosh(\eta-y)}{\sqrt{(M^2\cosh^2(\eta-y)-|\mathbf{q}_T|^2)}\sqrt{1-x^2}}\right)\right]\right\}_{-1}^{1} \\
&= \frac{\pi Q^2 M\cosh(\eta-y)}{4(M^2\cosh^2(\eta-y)-|\mathbf{q}_T|^2)^{3/2}}
\end{aligned} \tag{109}$$

We can go further and solve also the integral in η:

$$\begin{aligned}
&\int d^4p\,\delta(p^2)\delta((q-p)^2)\theta(p_0)\theta(q_0-p_0) = \int_{-\infty}^{\infty} d\eta \frac{\pi Q^2 M\cosh(\eta-y)}{4(M^2\cosh^2(\eta-y)-|\mathbf{q}_T|^2)^{3/2}} = \\
&\frac{\pi}{4}\frac{Q^2}{M^2}\int_{-\infty}^{\infty}\frac{d(\sinh\eta)}{\left(\sinh^2(\eta-y)+\frac{Q^2}{M^2}\right)^{3/2}} = \frac{\pi}{4}\frac{Q^2}{M^2}\left[\frac{M^2}{Q^2}\frac{\sinh\eta}{\sqrt{\sinh^2\eta+\frac{Q^2}{M^2}}}\right]_{-\infty}^{\infty} = \frac{\pi}{2}\,.
\end{aligned} \tag{110}$$

Remarkably, this result gives us the denominator of Eq. (94). We now need to compute the numerator by inserting the appropriate function Φ. In our case, the kinematic cuts are identical for the outgoing leptons and read:

$$\eta_{\min} < \eta_{1(2)} < \eta_{\max} \quad \text{and} \quad |\mathbf{p}_{T,1(2)}| > p_{T,\min}\,. \tag{111}$$

Therefore, the function Φ factorises into two identical functions as:

$$\Phi(p_1,p_2) = \Theta(p_1)\Theta(p_2)\,, \tag{112}$$

with:

$$\Theta(p) = \vartheta(\eta-\eta_{\min})\vartheta(\eta_{\max}-\eta)\vartheta(|\mathbf{p}_T|-p_{T,\min})\,. \tag{113}$$

Regerring to Eq. (94), and considering that:

$$q-p = (M\cosh y - |\mathbf{p}_T|\cosh\eta, \mathbf{q}_T - \mathbf{p}_T, M\sinh y - |\mathbf{p}_T|\sinh\eta)\,. \tag{114}$$

we thus have:

$$
\begin{aligned}
&\Phi(p,q-p)=\Theta(p)\Theta(q-p)= \\
&\vartheta(\eta-\eta_{\min})\vartheta(\eta_{\max}-\eta)\times \\
&\vartheta(|\mathbf{p}_T|-p_{T,\min})\times \\
&\vartheta\left(\frac{1}{2}\ln\left(\frac{M\cosh y-|\mathbf{p}_T|\cosh\eta+M\sinh y-|\mathbf{p}_T|\sinh\eta}{M\cosh y-|\mathbf{p}_T|\cosh\eta-M\sinh y+|\mathbf{p}_T|\sinh\eta}\right)-\eta_{\min}\right)\times \\
&\vartheta\left(\eta_{\max}-\frac{1}{2}\ln\left(\frac{M\cosh y-|\mathbf{p}_T|\cosh\eta+M\sinh y-|\mathbf{p}_T|\sinh\eta}{M\cosh y-|\mathbf{p}_T|\cosh\eta-M\sinh y+|\mathbf{p}_T|\sinh\eta}\right)\right)\times \\
&\vartheta(|\mathbf{q}_T-\mathbf{p}_T|-p_{T,\min})= \\
1):\quad &\vartheta(\eta-\eta_{\min})\times\vartheta(\eta_{\max}-\eta)\times \\
2):\quad &\vartheta(\overline{p}_T-p_{T,\min})\times \\
3):\quad &\vartheta\left(\frac{1}{2}\ln\left(\frac{Me^{y}-\overline{p}_Te^{\eta}}{Me^{-y}-\overline{p}_Te^{-\eta}}\right)-\eta_{\min}\right)\times\vartheta\left(\eta_{\max}-\frac{1}{2}\ln\left(\frac{Me^{y}-\overline{p}_Te^{\eta}}{Me^{-y}-\overline{p}_Te^{-\eta}}\right)\right)\times \\
4):\quad &\vartheta(\sqrt{|\mathbf{q}_T|^2+\overline{p}_T^2-2|\mathbf{q}_T|\overline{p}_T\cos\phi}-p_{T,\min})\,,
\end{aligned}
\tag{115}
$$

where in the last step we have replaced $|\mathbf{p}_T|$ with $\overline{p}_T$ defined Eq. (105). Now the question is identifying the integration domain defined by $\Phi(p,q-p)$ on the $(\eta,\cos\phi)$-plane. Since the θ-functions in Eq. (94) will be used inside a double nested integral over $x=\cos\phi$ first and η second, it is convenient to rewrite the function $\Phi(p,q-p)$ in Eq. (115) as follows:

$$
\begin{aligned}
\Phi(p,q-p) &= \vartheta(\eta-\eta_{\min})\times\vartheta(\eta_{\max}-\eta) \\
&\times\ \vartheta(x-f^{(2)}(\eta,p_{T,\min})) \\
&\times\ \vartheta(f^{(3)}(\eta,\eta_{\min})-x)\times\vartheta(f^{(3)}(\eta,\eta_{\max})-x) \\
&\times\ \vartheta(f^{(4)}(\eta,p_{T,\min})-x)\,,
\end{aligned}
\tag{116}
$$

with:

$$
\begin{aligned}
f^{(2)}(\eta,p_{T,\mathrm{cut}}) &= \frac{2Mp_{T,\min}\cosh(\eta-y)-Q^2}{2p_{T,\mathrm{cut}}|\mathbf{q}_T|}\,, \\
f^{(3)}(\eta,\eta_{\mathrm{cut}}) &= \frac{M\cosh(\eta-y)}{|\mathbf{q}_T|}-\frac{Q^2\left(\sinh(\eta-y)\coth(y-\eta_{\mathrm{cut}})+\cosh(\eta-y)\right)}{2|\mathbf{q}_T|M}\,, \\
f^{(4)}(\eta,p_{T,\mathrm{cut}}) &= \frac{M\cosh(\eta-y)(Q^2-2p_{T,\mathrm{cut}}^2+2|\mathbf{q}_T|^2)-Q^2\sqrt{M^2\sinh^2(\eta-y)+p_{T,\min}^2}}{2|\mathbf{q}_T|\left(M^2-p_{T,\min}^2\right)}\,.
\end{aligned}
\tag{117}
$$

Considering that $1\leq\cos\phi\leq 1$, the integration domain is limited to this region. Therefore, Eq. (116)

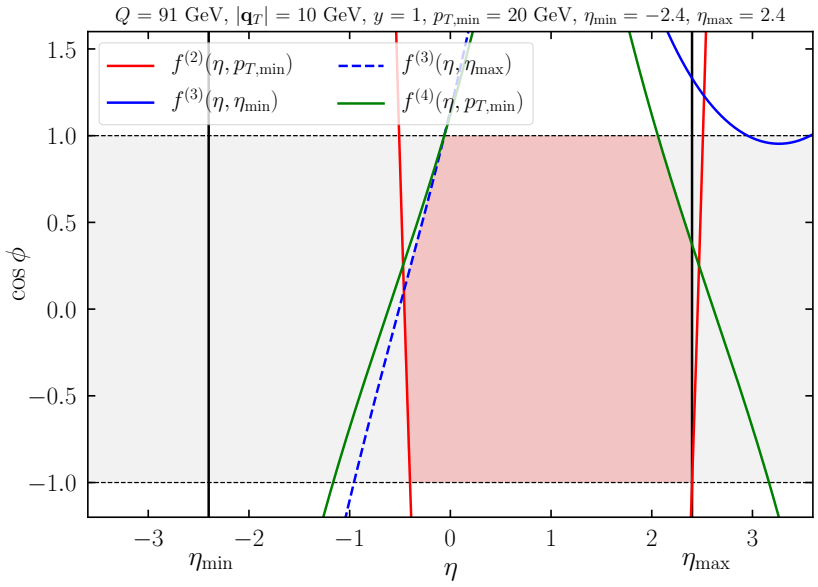

Figure 1: The red area indicates the integration domain of the numerator in of the phase-space reduction factor Eq. (94) for $p_{T,\min} = 20$ GeV and $-\eta_{\min} = \eta_{\max} = 2.4$ at $Q = 91$ GeV, $|\mathbf{q}_T| = 10$ GeV and $y = 1$.

can be written in an even more convenient way as:

$$\begin{aligned}\Phi(p, q-p) &= \vartheta(\eta - \eta_{\min})\vartheta(\eta_{\max} - \eta) \\ &\times \vartheta(x - \max[f^{(2)}(\eta, p_{T,\min}), -1]) \\ &\times \vartheta(\min[f^{(3)}(\eta, \eta_{\min}), f^{(3)}(\eta, \eta_{\max}), f^{(4)}(\eta, p_{T,\min}), 1] - x)\end{aligned} \tag{118}$$

such that a double integral over η and x would read:

$$\int_{-\infty}^{\infty} d\eta \int_{-1}^{1} dx\, \Phi(p, q-p) \cdots = \int_{\eta_{\min}}^{\eta_{\max}} d\eta\, \vartheta(x_2(\eta) - x_1(\eta)) \int_{x_1(\eta)}^{x_2(\eta)} dx \ldots . \tag{119}$$

with:

$$x_1(\eta) = \max[f^{(2)}(\eta, p_{T,\min}), -1] \tag{120}$$

and:

$$x_2(\eta) = \min[f^{(3)}(\eta, \eta_{\min}), f^{(3)}(\eta, \eta_{\max}), f^{(4)}(\eta, p_{T,\min}), 1]\,. \tag{121}$$

As an example, Fig. 1 shows the integration domain of the numerator in of the phase-space reduction factor Eq. (94) for $p_{T,\min} = 20$ GeV and $-\eta_{\min} = \eta_{\max} = 2.4$ at $Q = 91$ GeV, $|\mathbf{q}_T| = 10$ GeV and $y = 1$. The gray band corresponds to the region $1 \leq \cos\phi \leq 1$. The θ-function 1) in Eq. (115) limits the region to the vertical stip defined by $\eta_{\min} < \eta < \eta_{\max}$ (black vertical lines), the θ-function 2) gives the red lines, the θ-functions 3) the blue lines , and the θ-function 4) the green lines.

Gathering all pieces, the final expression for the phase-space reduction factor reads:

$$\mathcal{P}(Q, y, q_T) = \int_{\eta_{\min}}^{\eta_{\max}} d\eta\, \vartheta(x_2(\eta) - x_1(\eta))\, [F(x_2(\eta), \eta) - F(x_1(\eta), \eta)] \tag{122}$$

with:

$$F(x,\eta) = \frac{1}{4\pi}\frac{Q^2}{E_q^2-q_T^2}\left\{\frac{q_T^2 x\sqrt{1-x^2}}{x^2 q_T^2 - E_q^2}\right.$$
$$\left. - \frac{E_q}{\sqrt{E_q^2-q_T^2}}\left[\tan^{-1}\left(\frac{q_T - xE_q}{\sqrt{E_q^2-q_T^2}\sqrt{1-x^2}}\right) - \tan^{-1}\left(\frac{q_T + xE_q}{\sqrt{E_q^2-q_T^2}\sqrt{1-x^2}}\right)\right]\right\} \tag{123}$$

where we have defined $E_q = M\cosh(\eta - y)$ and $q_T = |\mathbf{q}_T|$.

Let us consider the case $y = q_T = 0$. For simplicity, we also take $\eta_{\min} = -\eta_{\max}$. In these conditions, Eq. (123) reduces to:

$$F(x,\eta) = \frac{1}{4\pi}\frac{1}{\cosh^2(\eta)}\left[\tan^{-1}\left(\frac{x}{\sqrt{1-x^2}}\right) - \tan^{-1}\left(-\frac{x}{\sqrt{1-x^2}}\right)\right] . \tag{124}$$

As evident from Eq. (117), for $q_T = 0$ all functions $f^{(2)}$, $f^{(3)}$, and $f^{(4)}$ diverge. The relevant question, though, is whether they go to plus or minus infinity depending on the value of Q. Of course, q_T will tend to zero positively so we find:

$$\begin{aligned}
&f^{(2)}(\eta, p_{T,\min}) \to \infty \times \text{sign}\left[2p_{T,\min}\cosh(\eta) - Q\right] ,\\
&f^{(3)}(\eta, \eta_{\min} = -\eta_{\max}) \to +\infty\\
&f^{(3)}(\eta, \eta_{\max}) \to -\infty ,\\
&f^{(4)}(\eta, p_{T,\min}) \to \infty \times \text{sign}\left[\frac{\cosh(\eta)(Q^2 - 2p_{T,\min}^2) - Q\sqrt{Q^2\sinh^2(\eta) + p_{T,\min}^2}}{Q^2 - p_{T,\min}^2}\right] ,
\end{aligned} \tag{125}$$

Therefore, $f^{(3)}$ never actually contributes. In addition, for the θ-function in Eq. (122) to be different from zero, we need $f^{(2)}(\eta) \to -\infty$ and $f^{(3)}(\eta) \to \infty$. These both translate into $Q \geq 2p_{T,\min}\cosh(\eta)$. This inequality is satisfied only if $Q \geq 2p_{T,\min}$ for:

$$-\overline{\eta} \leq \eta \leq \overline{\eta} \quad \text{with} \quad \overline{\eta} = \cosh^{-1}\left(\frac{Q}{2p_{T,\min}}\right) . \tag{126}$$

Therefore, the phase-space reduction factor eventually becomes:

$$\begin{aligned}
\mathcal{P}(Q,0,0) &= \frac{1}{2}\vartheta(Q - 2p_{T,\min})\int_{-\eta_{\max}}^{\eta_{\max}}\frac{d\eta}{\cosh^2\eta}\,\vartheta(\eta+\overline{\eta})\vartheta(\overline{\eta}-\eta)\\
&= \vartheta(Q - 2p_{T,\min})\tanh(\max[\eta_{\max},\overline{\eta}]) .
\end{aligned} \tag{127}$$

This result can be written more explicitly as:

$$\mathcal{P}(Q,0,0) = \begin{cases} 0 & Q < 2p_{T,\min} ,\\ \tanh(\overline{\eta}) = \left(1 + \dfrac{2p_{T,\min}}{Q}\right)\sqrt{1 - \dfrac{4p_{T,\min}}{Q + 2p_{T,\min}}} & 2p_{T,\min} \leq Q < 2p_{T,\min}\cosh\eta_{\max} ,\\ \tanh(\eta_{\max}) & Q \geq 2p_{T,\min}\cosh\eta_{\max} . \end{cases} \tag{128}$$

This differs from Eq. (24) of Ref. [1]. Despite the three different regions coincide, the behavior of the phase-space reduction factor for all regions but for $Q < 2p_{T,\min}$ is different. In favour of our result there is the fact that $\mathcal{P}(Q,0,0)$ in Eq. (128) is continuous at $Q = 2p_{T,\min}\cosh\eta_{\max}$ while that of Ref. [1] is not. In addition, when setting $p_{T,\min} = 0$ and $\eta_{\max} = \infty$, *i.e.* no cuts, our result tends to

$\mathcal{P}(Q,0,0) = \tanh(\infty) = 1$, as it should. While the result in Eq. (24) of Ref. [1] actually diverges in this limit.

The integrand of Eq. (122), due to the behaviour of x_1 and x_2 as functions of η, a piecewise function. Therefore, its numerical integration is problematic in that quadrature algorithms assume the integrand be continuos over the integration range. The solution is to identify the discontinuity points and integrate the function separately over the resulting ranges. However, the complexity of the integration region (*e.g.* see Fig. 1) makes the analytical identification of the discontinuity points very hard to achieve.

C.1 Contracting the leptonic tensor with $g_\perp^{\mu\nu}$

The calculation done in the previous section holds when contracting the leptonic tensor $L_{\mu\nu}$ with the metric tensor $g^{\mu\nu}$ associated with the Lorentz structure of the hadronic tensor. However, at small values of $|\mathbf{q}_T|$, the leading-power Lorentz structure that one needs to multiply the leptonic tensor for is:

$$g_\perp^{\mu\nu} = g^{\mu\nu} + z^\mu z^\nu - t^\mu t^\nu \tag{129}$$

where the vectors z^μ and t^μ in the Collins-Soper (CS) frame are defined as:

$$\begin{aligned} z^\mu &= (\sinh y, \mathbf{0}, \cosh y)\,, \\ t^\mu &= \frac{q^\mu}{Q}\,, \end{aligned} \tag{130}$$

and they are such that $z^2 = -1$, $t^2 = 1$ and $zq = 0$. if we use the on-shell-ness of p_1 and p_2 ($p_1^2 = p_2^2 = 0$) and the momentum conservation ($p \equiv p_1$, $p_2 = q - p$), we find that $t^\mu t^\nu L_{\mu\nu} = 0$ and the quantity above reduces to:

$$L_\perp = g_\perp^{\mu\nu} L_{\mu\nu} = 4\left[\frac{1}{2}q^2 + 2(zp)^2\right] = 2Q^2\left[1 + 4\sinh^2(y-\eta)\frac{|\mathbf{p}_T|^2}{Q^2}\right]. \tag{131}$$

Therefore, we need to introduce this factor in both the numerator and the denominator of Eq. (94). Following the same steps of the previous section, up to a factor $2Q^2$, this leads us to replace the integral in Eq. (104) with([9]):

$$\frac{1}{2}\int_0^\infty |\mathbf{p}_T|\left[1 + 4\sinh^2(y-\eta)\frac{|\mathbf{p}_T|^2}{Q^2}\right] d|\mathbf{p}_T|\,\delta(Q^2 - 2p\cdot q) = \frac{2\overline{p}_T^2}{Q^2} + 2\sinh^2(y-\eta)\frac{\overline{p}_T^4}{Q^4}\,. \tag{132}$$

We can still use Eq. (107) for the first term in the r.h.s. of the equation above. For the second, instead we need to use:

$$\begin{aligned} \int \frac{dx}{(a\pm x)^4\sqrt{1-x^2}} &= \frac{\sqrt{1-x^2}\left[(11a^2+4)x^2 \pm 3a(9a^2+1)x + (18a^4 - 5a^2 + 2)\right]}{6(a^2-1)^3(x\pm a)^3} \\ &\pm \frac{a(2a^2+3)}{2(a^2-1)^{7/2}}\tan^{-1}\left(\frac{1\pm ax}{\sqrt{a^2-1}\sqrt{1-x^2}}\right), \end{aligned} \tag{133}$$

that is such that:

$$\int_{-1}^1 \frac{dx}{(a\pm x)^4\sqrt{1-x^2}} = \frac{\pi a(2a^2+3)}{2(a^2-1)^{7/2}}\,. \tag{134}$$

In our particular case, the integrand we are considering is the second term in the r.h.s. term of Eq. (132):

$$\begin{aligned} &\frac{2\sinh^2(y-\eta)}{Q^4}\int_{-1}^1 d(\cos\phi)\overline{p}_T^4(\cos\phi) = \\ &\frac{Q^4}{8q_T^4}\sinh^2(y-\eta)\int_{-1}^1 \frac{dx}{\sqrt{1-x^2}}\left[\frac{1}{(a+x)^4} + \frac{1}{(a-x)^4}\right] = \frac{\pi Q^4}{8q_T^4}\sinh^2(y-\eta)\frac{a(2a^2+3)}{(a^2-1)^{7/2}}\,. \end{aligned} \tag{135}$$

[9] We removed the θ-function as we know it does not have any effect.

with:

$$a = \frac{M}{q_T}\cosh(y-\eta)\,. \tag{136}$$

Now we need to integrate Eq. (135) over η:

$$\frac{\pi Q^4}{8q_T^4}\int_{-\infty}^{\infty} d\eta \sinh^2(y-\eta)\frac{a(2a^2+3)}{(a^2-1)^{7/2}}\,. \tag{137}$$

If we make the following change of variable in the integral above:

$$z = \frac{M}{q_T}\sinh(y-\eta) \tag{138}$$

such that:

$$a^2 = z^2 + \frac{M^2}{q_T^2} \quad \text{and} \quad dz = -a d\eta\,, \tag{139}$$

the integral above becomes:

$$\frac{\pi Q^4}{4M^2q_T^2}\int_{-\infty}^{\infty} dz \frac{z^2\left(z^2+\frac{M^2}{q_T^2}+\frac{3}{2}\right)}{\left(z^2+\frac{M^2}{q_T^2}-1\right)^{7/2}} = \frac{\pi}{6}\,. \tag{140}$$

Putting this result together with Eq. (110) and taking into account the factor $2Q^2$ in Eq. (131), we find that:

$$\int d^4p\delta(p^2)\delta((q-p)^2)\theta(p_0)\theta(q_0-p_0)L_\perp = \frac{4\pi}{3}Q^2\,. \tag{141}$$

This result agrees with Eq. (2.38) of Ref. [1], up to a factor four. This provides the denominator of the phase-space-reduction factor $\mathcal{P}$. The structure of $\mathcal{P}$ will be exactly like that in Eq. (122), the only thing we need to do is to identify the correct function $F(x,\eta)$. To this end, we need to make the following replacement for the function F given in Eq. (123) with:

$$F(x,\eta) \to \overline{F}(x,\eta) = \frac{3}{4}F(x,\eta) + \frac{1}{4}G(x,\eta)\,, \tag{142}$$

where:

$$\begin{aligned}
G(x,\eta) &= \frac{1}{16\pi}\sinh^2(y-\eta)\frac{Q^4}{(E_q^2-q_T^2)^3}\Bigg\{\sqrt{1-x^2}q_T \\
&\times \Bigg[\frac{(11E_q^2q_T^2+4q_T^4)x^2+3E_qq_T(9E_q^2+q_T^2)x+(18E_q^4-5E_q^2q_T^2+2q_T^4)}{(xq_T+E_q)^3} \\
&+ \frac{(11E_q^2q_T^2+4q_T^4)x^2-3E_qq_T(9E_q^2+q_T^2)x+(18E_q^4-5E_q^2q_T^2+2q_T^4)}{(xq_T-E_q)^3}\Bigg] \\
&- \frac{6E_q(2E_q^2+3q_T^2)}{\sqrt{E_q^2-q_T^2}}\left[\tan^{-1}\left(\frac{q_T-xE_q}{\sqrt{E_q^2-q_T^2}\sqrt{1-x^2}}\right)-\tan^{-1}\left(\frac{q_T+xE_q}{\sqrt{E_q^2-q_T^2}\sqrt{1-x^2}}\right)\right]\Bigg\}\,.
\end{aligned} \tag{143}$$

Finally, combining the functions F and G given in Eqs. (123) and (143), respectively, according to Eq. (142) to obtain $\overline{F}$, and replacing F with $\overline{F}$ in Eq. (122) gives the phase-space-reduction factor $\mathcal{P}(Q,y,q_T)$ when the leptonic tensor $L_{\mu\nu}$ is contracted with the transverse metrics $g_\perp^{\mu\nu}$.

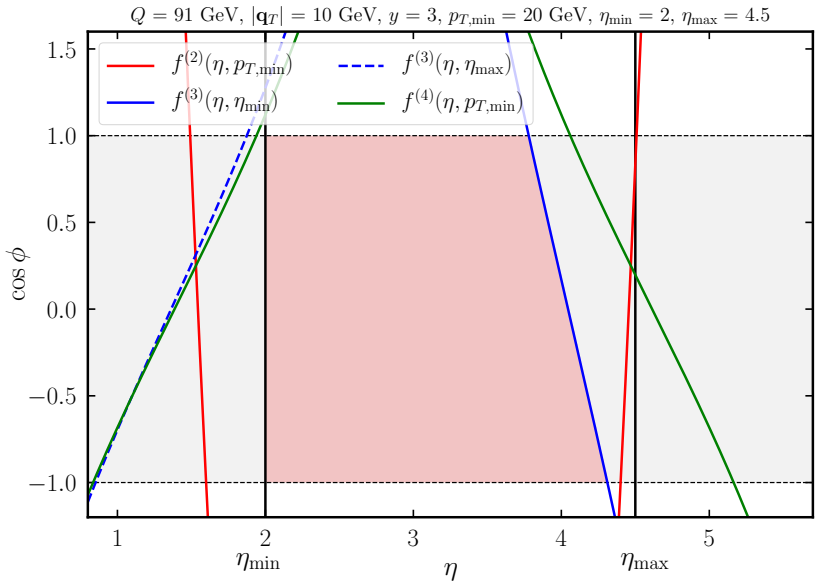

Figure 2: Same as Fig. 1 for the asymmetric rapidity cut $2 < \eta < 4.5$ at $y = 3$.

As a final check, it is interesting to compute $\mathcal{P}$ when $y = q_T = 0$, again assuming $\eta_{\min} = -\eta_{\max}$. In this limit F reduces to the expression in Eq. (124), while G becomes:

$$G(x,\eta) = \frac{3}{4\pi}\frac{\sinh^2(\eta)}{\cosh^4(\eta)}\left\{\left[\tan^{-1}\left(\frac{x}{\sqrt{1-x^2}}\right) - \tan^{-1}\left(-\frac{x}{\sqrt{1-x^2}}\right)\right]\right\}, \tag{144}$$

such that:

$$\begin{aligned}\mathcal{P}(Q,0,0) &= \frac{3}{8}\vartheta(Q-2p_{T,\min})\int_{-\eta_{\max}}^{\eta_{\max}} d\eta\left[\frac{\cosh^2(\eta)+\sinh^2(\eta)}{\cosh^4(\eta)}\right]\vartheta(\eta+\overline{\eta})\vartheta(\overline{\eta}-\eta) \\ &= \vartheta(Q-2p_{T,\min})\tanh(\max[\eta_{\max},\overline{\eta}])\left[1-\frac{1}{4\cosh^2(\max[\eta_{\max},\overline{\eta}])}\right],\end{aligned} \tag{145}$$

with $\overline{\eta}$ defined in Eq. (126). The relation above can be written more explicitly as:

$$\mathcal{P}(Q,0,0) = \begin{cases} 0 & Q < 2p_{T,\min}\,, \\ \tanh(\overline{\eta})\left[1-\frac{1}{4\cosh^2(\overline{\eta})}\right] = \left(1-\frac{p_{T,\min}^2}{Q^2}\right)\sqrt{1-\frac{4p_{T,\min}^2}{Q^2}} & 2p_{T,\min} \le Q < 2p_{T,\min}\cosh\eta_{\max}\,, \\ \tanh(\eta_{\max})\left[1-\frac{1}{4\cosh^2(\eta_{\max})}\right] & Q \ge 2p_{T,\min}\cosh\eta_{\max}\,. \end{cases} \tag{146}$$

The reason why we kept $\eta_{\min} \neq -\eta_{\max}$ is that in some cases it may be required to implement an asymmetric cut, $\eta_{\min} < \eta < \eta_{\max}$. This is the case, for example, of the LHCb experiment that delivers data only in the forward region ($2 < \eta < 4.5$). As an example, Fig. 2 shows the integration domain of the phase-space reduction factor Eq. (94) for $p_{T,\min} = 20$ GeV and $2 < \eta < 4.5$ at $Q = 91$ GeV, $|\mathbf{q}_T| = 10$ GeV and $y = 3$.

C.2 Parity-violating contribution

In the presence of cuts on the final-state leptons and for invariant masses around the Z mass, parity-violating effects arise. As we will show below, these effects integrate to zero when removing the

leptonic cuts. This contribution stems from interference of the antisymmetric contributions to the lepton tensor, proportional to $p_1^\mu p_2^\nu \epsilon_{\mu\nu\rho\sigma}$, and the hadronic tensor, proportional to $\epsilon_\perp^{\mu\nu}$ defined as:

$$\epsilon_\perp^{\mu\nu} \equiv \epsilon^{\mu\nu\rho\sigma} t_\rho z_\sigma \,, \tag{147}$$

where t^μ and z^μ are given in Eq. (130). Therefore, the contribution we are after results from the contraction of the following Lorentz structures:

$$L_{\rm PV} \equiv p_1^\mu p_2^\nu \epsilon_{\mu\nu\rho\sigma} \epsilon_\perp^{\rho\sigma} \,. \tag{148}$$

After some manipulation, one finds:

$$\begin{aligned} L_{\rm PV} &= p_1^\mu p_2^\nu \epsilon_{\mu\nu\rho\sigma} \epsilon^{\rho\sigma\alpha\beta} t_\alpha z_\beta = -2 p_1^\mu p_2^\nu \delta_\mu^\alpha \delta_\nu^\beta t_\alpha \\ &= -2(p_1 t)(p_2 z) = -2(pt)\left[(qz) - (pz)\right] = 2(pt)(pz) \\ &= \frac{2|\mathbf{p}_T|^2}{Q} \sinh(y-\eta) \left[M \cosh(y-\eta) - |\mathbf{q}_T| \cos\phi\right] \,, \end{aligned} \tag{149}$$

where I have defined $p_1 \equiv p$ and used the equalities $p_2 = q - p$, and $zq = 0$. To compute the third line I have used the explicit parameterisation of q and p given in Eqs. (100) and (101), respectively. The presence of $\sinh(y-\eta)$ in Eq. (149) is such that integrating over the full range in the lepton rapidity η nullifies this contribution:

$$\int_{-\infty}^{\infty} d\eta \, L_{\rm PV} = 0 \,. \tag{150}$$

Therefore, it turns out that, for observables inclusive in the lepton phase space, the parity violating term does not give any contribution. Conversely, the presence of cuts on the final-state leptons may prevent Eq. (150) from being satisfied leaving a residual contribution. In order to quantify this effect, we take the same steps performed in the previous sections to integrate $L_{\rm PV}$ over the fiducial region. As above, we start integrating over the full range in $|\mathbf{p}_T|$ using the on-shell-ness δ-function:

$$\begin{aligned} \int_0^\infty d|\mathbf{p}_T| |\mathbf{p}_T| \, L_{\rm PV} &= \frac{\sinh(y-\eta)}{Q} \left[M \cosh(y-\eta) - |\mathbf{q}_T| \cos\phi\right] \int_0^\infty d|\mathbf{p}_T| |\mathbf{p}_T|^3 \delta(Q^2 - 2pq) \\ &= \frac{\overline{p}_T^4}{Q^3} \sinh(y-\eta) \left[M \cosh(y-\eta) - |\mathbf{q}_T| \cos\phi\right] \,, \end{aligned} \tag{151}$$

with $\overline{p}_T$ defined in Eq. (105). Now we compute the indefinte integral over $\cos\phi$. To do so, we need to use Eq. (106) along with the equality:

$$\int \frac{dx}{(a \pm x)^3 \sqrt{1-x^2}} = \frac{\sqrt{1-x^2}\left[3ax \pm (4a^2-1)\right]}{2(a^2-1)^2 (x \pm a)^2} \pm \frac{(2a^2+1)}{2(a^2-1)^{5/2}} \tan^{-1}\left(\frac{1 \pm ax}{\sqrt{a^2-1}\sqrt{1-x^2}}\right) \,. \tag{152}$$

This allows us to compute the integral([10]):

$$
\begin{aligned}
H(x,\eta) &= \left(\frac{4\pi Q^2}{3}\right)^{-1} \frac{\sinh(y-\eta)}{Q^3}\left[M\cosh(y-\eta)\int d(\cos\phi)\overline{p}_T^4(\cos\phi) - |\mathbf{q}_T|\int d(\cos\phi)\cos\phi\,\overline{p}_T^4(\cos\phi)\right] \\
&= \frac{3Q^3\sinh(y-\eta)}{64\pi|\mathbf{q}_T|^4}\left[M\cosh(y-\eta)\int \frac{d(\cos\phi)}{(a-\cos\phi)^4} - |\mathbf{q}_T|\int \frac{\cos\phi\, d(\cos\phi)}{(a-\cos\phi)^4}\right] \\
&= \frac{3Q^3\sinh(y-\eta)}{64\pi q_T^3}\int \frac{dx}{\sqrt{1-x^2}}\left[\frac{1}{(a-x)^3}+\frac{1}{(a+x)^3}\right] \\
&= \frac{3Q^3\sinh(y-\eta)}{128\pi q_T^3}\left\{\frac{\sqrt{1-x^2}}{(a^2-1)^2}\left[\frac{3ax-(4a^2-1)}{(x-a)^2}+\frac{3ax+(4a^2-1)}{(x+a)^2}\right]\right. \\
&- \left.\frac{(2a^2+1)}{(a^2-1)^{5/2}}\left[\tan^{-1}\left(\frac{1-ax}{\sqrt{a^2-1}\sqrt{1-x^2}}\right)-\tan^{-1}\left(\frac{1+ax}{\sqrt{a^2-1}\sqrt{1-x^2}}\right)\right]\right\}
\end{aligned}
\tag{153}
$$

with $E_q = M\cosh(\eta - y)$, $q_T = |\mathbf{q}_T|$, and:

$$
a = \frac{E_q}{q_T}\,, \tag{154}
$$

so that:

$$
\begin{aligned}
H(x,\eta) &= \frac{3Q^3\sinh(y-\eta)}{128\pi(E_q^2-q_T^2)^2}\left\{\sqrt{1-x^2}q_T\left[\frac{3E_qq_Tx-(4E_q^2-q_T^2)}{(xq_T-E_q)^2}+\frac{3E_qq_Tx+(4E_q^2-q_T^2)}{(q_Tx+E_q)^2}\right]\right. \\
&- \left.\frac{(2E_q^2+q_T^2)}{\sqrt{E_q^2-q_T^2}}\left[\tan^{-1}\left(\frac{q_T-xE_q}{\sqrt{E_q^2-q_T^2}\sqrt{1-x^2}}\right)-\tan^{-1}\left(\frac{q_T+xE_q}{\sqrt{E_q^2-q_T^2}\sqrt{1-x^2}}\right)\right]\right\}.
\end{aligned}
\tag{155}
$$

Finally, using the definition of H in Eq. (155), one can perform the integral over the fiducial phase space as discussed above in Eq. (122):

$$
\mathcal{P}_{\rm PV}(Q,y,q_T) = \int_{\eta_{\rm min}}^{\eta_{\rm max}} d\eta\,\vartheta(x_2(\eta)-x_1(\eta))\left[H(x_2(\eta),\eta)-H(x_1(\eta),\eta)\right]\,. \tag{156}
$$

This allows one to estimate the impact of the parity-violating contribution to the phase-space reduction factor.

In order to quantify numerically the impact of Eq. (156), Fig. 3 displays the size $\mathcal{P}_{\rm PV}$ relative to the parity-conserving phase-space reduction factor as a function of y for three different values of q_T at $Q = M_Z$ and for the following lepton cuts: $p_{T,\ell} > 20$ GeV and $-2.4 < \eta_\ell < 2.4$. It turns out that the size of $\mathcal{P}_{\rm PV}$ relative to $\mathcal{P}$ is never larger than 2×10^{-6}. In addition, the rapid oscillations with y contribute to suppress even more the integral over realistic bins in y. One can thus conclude that, for realistic kinematic configurations, the impact of parity violating effects is completely negligible.

D Differential cross section in the leptonic variables

The calculation of the phase-space reduction factor carried out in the previous section can be used to express the Drell-Yan cross section in Eq.(1) as differential in the kinematic variables of the single

[10] The factor $\left(\frac{4\pi Q^2}{3}\right)^{-1}$ in Eq. (153) corresponds to the full phase-space in integral of $L_\perp$ in Eq. (141) that provides the natural normalisation.

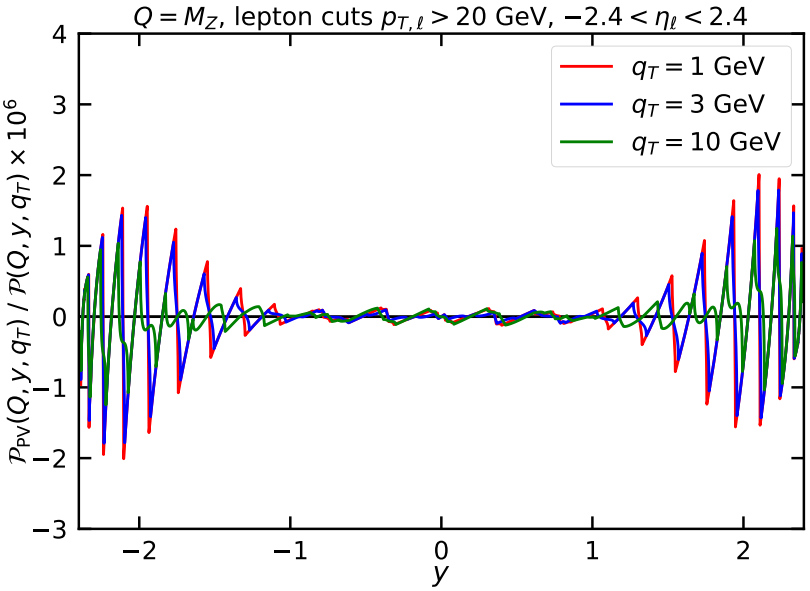

Figure 3: Ratio between the parity-violating phase-space reduction factor $\mathcal{P}_{\rm PV}$ in Eq. (156) and the respective parity-conserving factor as a function of the Z rapidity y at $Q = M_Z$ and for three different values of q_T, with lepton cuts equal to $p_{T,\ell} > 20$ GeV and $-2.4 < \eta_\ell < 2.4$.

leptons. Loosely speaking, this amounts to removing the integral sign in the numerator in Eq. (88) but taking into account kinematic constraints. Using the transverse metric tensor $g_\perp^{\mu\nu}$, one finds:

$$d\mathcal{P} = \frac{d^4p_1 d^4p_2\, \delta(p_1^2)\delta(p_2^2)\theta(p_{1,0})\theta(p_{2,0})\delta^{(4)}(p_1+p_2-q)L_\perp(p_1,p_2)}{\displaystyle\int d^4p_1 d^4p_2\, \delta(p_1^2)\delta(p_2^2)\theta(p_{1,0})\theta(p_{2,0})\delta^{(4)}(p_1+p_2-q)L_\perp(p_1,p_2)}\,, \tag{157}$$

From Eq. (141), we know the value of the denominator. In the numerator, we can make use of the momentum-conservation and one of the on-shell-ness δ-functions. Using the r.h.s. of Eq. (132), but integrating over ϕ rather than $|\mathbf{p}_T|$, leads to:

$$\frac{d\mathcal{P}}{d|\mathbf{p}_T|d\eta} = \frac{3|\mathbf{p}_T|}{4\pi}\left[1 + 4\sinh^2(y-\eta)\frac{|\mathbf{p}_T|^2}{Q^2}\right]\int_0^{2\pi} d\phi\, \delta(Q^2 - 2|\mathbf{p}_T|\left[M\cosh(\eta - y) - |\mathbf{q}_T|\cos\phi\right])\,, \tag{158}$$

where we have used Eqs. (95)-(99) and Eq. (103). Finally, to perform the integral over ϕ we use Eq. (106) to get:

$$\frac{d\mathcal{P}}{d|\mathbf{p}_T|d\eta} = \frac{3|\mathbf{p}_T|}{2\pi Q^2}\frac{Q^2 + 4|\mathbf{p}_T|^2\sinh^2(\eta - y)}{\sqrt{4|\mathbf{p}_T|^2|\mathbf{q}_T|^2 - (2|\mathbf{p}_T|M\cosh(\eta-y) - Q^2)^2}}\,. \tag{159}$$

Getting rid of the absolute value of the transverse vectors, this allows one to get the Drell-Yan cross section differential in the leptonic variables $|\mathbf{p}_T|$ and η:

$$\frac{d\sigma}{dQdydq_Td\eta dp_T} = \left[\frac{3p_T^2}{\pi Q^2 M}\frac{\left(\frac{Q^2}{4p_T^2} - 1\right) + \cosh^2(\eta - y)}{\sqrt{\frac{q_T^2}{M^2} - \left(\cosh(\eta - y) - \frac{Q^2}{2p_T M}\right)^2}}\right]\frac{d\sigma}{dQdydq_T}\,. \tag{160}$$

Due to the square root in the denominator, for fixed values of Q, q_T, and y, the expression above is defined for values of p_T and η such that:

$$\frac{Q^2}{2p_T M} - \frac{q_T}{M} < \cosh(\eta - y) < \frac{Q^2}{2p_T M} + \frac{q_T}{M}\,. \tag{161}$$

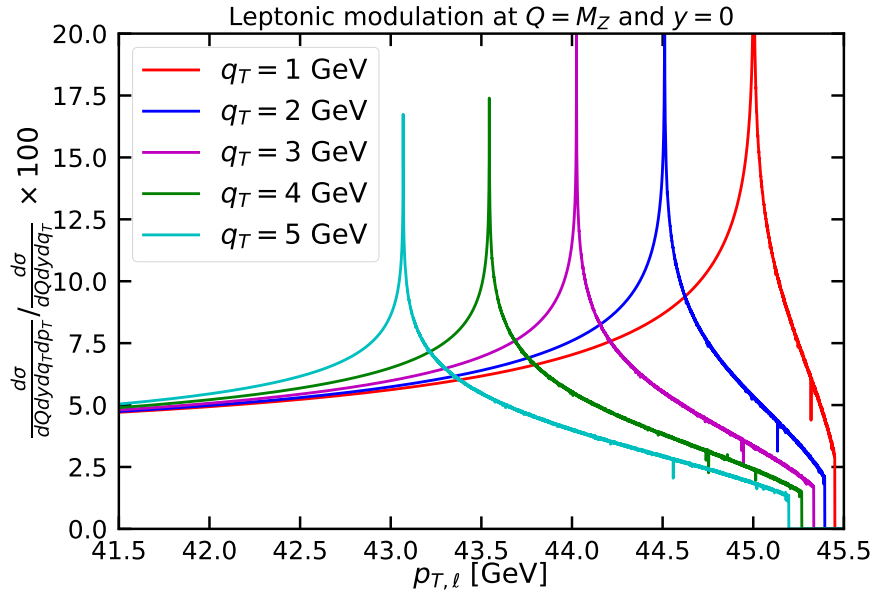

Figure 4: Behaviour of the second line of Eq. (163) at $Q = M_Z$ and $y = 0$ as a function of the lepton transverse momentum $p_{T,\ell}$.

In order to focus on the p_T dependence of the cross section, one may want to integrate of the lepton rapidity η. Using the analogous of Eq. (106) for $\cosh(\eta)$:

$$\int_{-\infty}^{\infty} d\eta\, f(\cos\eta) = \int_{1}^{\infty} \frac{dx}{\sqrt{x^2-1}} \left[f(x) + f(-x)\right] , \tag{162}$$

and taking into account the constraint in Eq. (161), one finds:

$$\begin{aligned} \frac{d\sigma}{dQdydq_Tdp_T} &= \frac{d\sigma}{dQdydq_T} \times \\ \frac{3p_T}{2\pi Q^2} \int_{-\frac{q_T}{M}}^{\frac{q_T}{M}} \frac{dy}{\sqrt{\frac{q_T^2}{M^2} - y^2}} &\left(\frac{\left(\frac{Q^2}{4p_T^2} - 1\right) + \left(y + \frac{Q^2}{2p_T M}\right)^2}{\sqrt{\left(y + \frac{Q^2}{2p_T M}\right)^2 - 1}} + \frac{\left(\frac{Q^2}{4p_T^2} - 1\right) + \left(y - \frac{Q^2}{2p_T M}\right)^2}{\sqrt{\left(y - \frac{Q^2}{2p_T M}\right)^2 - 1}} \right) . \end{aligned} \tag{163}$$

For fixed values of Q, q_T, and y, the integral above can be solved numerically a plotted as a function of p_T. The result is shown in Fig. 4.

References

[1] I. Scimemi and A. Vladimirov, arXiv:1706.01473 [hep-ph].

[2] J. Collins, Camb. Monogr. Part. Phys. Nucl. Phys. Cosmol. **32** (2011) 1.

[3] H. Ogata, "A Numerical Integration Formula Based on the Bessel Functions," http://www.kurims.kyoto-u.ac.jp/∼okamoto/paper/Publ_RIMS_DE/41-4-40.pdf